DALHOUSIE UNIVERSITY
Inspiring Minds

DID THE ADULA NAPPE (EUROPEAN BASEMENT) ENDURE UHP METAMORPHISM DURING THE ALPINE OROGENY?
INSIGHT FROM A (MICRO)STRUCTURAL AND TEXTURAL STUDY

Svieda Ma

SUBMITTED IN PARTIAL FULFILLMENT OF THE REQUIREMENTS FOR THE
DEGREE OF BACHELOR OF SCIENCES, HONOURS
DEPARTMENT OF EARTH SCIENCES
DALHOUSIE UNIVERSITY, HALIFAX, NOVA SCOTIA
APRIL 2014

Distribution License

DalSpace requires agreement to this non-exclusive distribution license before your item can appear on DalSpace.

NON-EXCLUSIVE DISTRIBUTION LICENSE

You (the author(s) or copyright owner) grant to Dalhousie University the non-exclusive right to reproduce and distribute your submission worldwide in any medium.

You agree that Dalhousie University may, without changing the content, reformat the submission for the purpose of preservation.

You also agree that Dalhousie University may keep more than one copy of this submission for purposes of security, back-up and preservation.

You agree that the submission is your original work, and that you have the right to grant the rights contained in this license. You also agree that your submission does not, to the best of your knowledge, infringe upon anyone's copyright.

If the submission contains material for which you do not hold copyright, you agree that you have obtained the unrestricted permission of the copyright owner to grant Dalhousie University the rights required by this license, and that such third-party owned material is clearly identified and acknowledged within the text or content of the submission.

If the submission is based upon work that has been sponsored or supported by an agency or organization other than Dalhousie University, you assert that you have fulfilled any right of review or other obligations required by such contract or agreement.

Dalhousie University will clearly identify your name(s) as the author(s) or owner(s) of the submission, and will not make any alteration to the content of the files that you have submitted.

If you have questions regarding this license please contact the repository manager at dalspace@dal.ca.

Grant the distribution license by signing and dating below.

_____ _____

Name of signatory Date

DALHOUSIE UNIVERSITY
Inspiring Minds

Department of Earth Sciences
Halifax, Nova Scotia
Canada B3H 4R2
(902) 494-2358
Fax (902) 494-6889

DATE: 22 April 2014

AUTHOR: Svieda Ma

TITLE: Did the Adula nappe (European basement) endure UHP metamorphism during the Alpine Orogeny? Insight from a (micro)structural and textural study

Degree: B. Sc. Hons. Earth Sciences Convocation: May Year: 2014

Abstract

The mafic-ultramafic rocks in the Adula nappe and its westernmost Cima Lunga unit preserve the only record of regional high- to ultrahigh-pressure metamorphism (~13-35 kbar) in the Central Alps. These rocks are contained within felsic country rock gneisses, which are up to 25 kbar lower in peak-pressure conditions. The Adula-Cima Lunga nappe is traditionally interpreted as a tectonic mélange of the European continental basement, metasediments and metavolcanics of Valais ocean- and mantle-derived ultramafic rocks. The exhumation and emplacement of ultrahigh-pressure (UHP) rocks into lower-pressure units remains enigmatic; even more so is the subduction of a large piece of continental crust to mantle depths. This study investigates the kinematics of (U)HP eclogites and the surrounding country rocks in the Cima Lunga unit through structural mapping and a microstructural and textural analysis. Structural mapping allows for a re-interpretation of the lower Cima Lunga nappe boundary. Paired with structural and textural observations, the mafic-ultramafic (U)HP rocks are presented here as a nappe separating lithology rather than lenses within a basement nappe unit.

We examine the lattice preferred orientation in omphacite using electron backscatter diffraction to determine the deformation regime active under (U)HP conditions. Our microstructural observations reveal limited evidence for simple shear; instead, textural data of eclogite rocks show affinity for a flattening strain geometry. When comparing our textural observations with published data from the Cima Lunga and the main Adula nappe, we consistently observe a contrast in omphacite texture between the two areas. Geochronological and thermobarometric data from published studies show similar contrasts: the main Adula nappe has experienced two orogenic cycles of (U)HP subduction and exhumation, while the Cima Lunga has only experienced one cycle during the Alpine orogeny. Structural position, age, and textural discrepancies between the main Adula nappe and the Cima Lunga unit leads us to suggest that these two units have experienced a different geodynamic history and can be considered as two separate lithotectonic units. In summary, I suggest that only the ultramafic rocks of the Cima Lunga domain have endured UHP metamorphism (> 30 kbar), while the Adula nappe was subducted during Alpine orogeny as a coherent body to maximum depths of “only” 24 kbar.

Keywords: Adula nappe, Cima Lunga, eclogite, UHP metamorphism, omphacite LPO, Alpine orogeny

Table of Contents

Abstract ii

Table of Contents iii

Table of Figures v

List of Abbreviations vii

Acknowledgements viii

Chapter 1: Introduction 1

1.1 Scope of this study 3

Chapter 2: Geological Background 4

2.1 Introduction to the Alpine Framework 4

2.1.1 Large Scale Structures and Units 6

2.1.1.1 European Plate 8

2.1.1.2 Adria Plate 9

2.2 Adula Nappe 10

2.2.1 Field Area 10

2.2.2 Petrography 11

2.2.3 Deformation History 13

2.2.4 Metamorphic Conditions and Geochronological Data 16

2.3 Unresolved Geological Problems 19

2.3.1 Motivation for Study 21

Chapter 3: Methods 23

3.1 Field Methods 23

3.2 Optical Microscopy 25

3.3 Electron Back-scatter Diffraction 26

3.3.1 Sample Preparation 28

3.3.2 Instrumentation 28

3.4 Lattice Preferred Orientation 29

3.4.1 Omphacite LPO 31
Chapter 4: Map Structures and Microstructures 34
4.1 Map-scale Structures 34
4.1.1 Field Observations 34
4.1.2 Discussion 37
4.1.3 Reinterpretation of the Simano–Cima Lunga Nappe Contact 39
4.2 Microstructures 42
4.2.1 Microstructural observations 42
4.2.2 Discussion 49
4.3 Summary of (Micro)structural Observations 49
Chapter 5: Textures 51
5.1 ESBD Results 51
5.2 Discussion 54
5.3 Textural Contrast between the Adula and Cima Lunga Units 55
5.4 Tectonic Implications 55
Chapter 6: Conclusions and Recommendations 58
6.1 Conclusions 58
6.2 Recommendations for Further Study 59
References 61
Appendix A 68

Table of Figures

Chapter 1: Introduction

Figure 1.1 Simplified P-T facies diagram defining UHP and HP conditions 1

Figure 1.2 Global distribution of UHP metamorphic terranes 2

Chapter 2: Geological Background

Figure 2.1 Simplified tectonic map of the Alpine system 4

Figure 2.2 Paleogeography of the Central Alps 5

Figure 2.3 Schematic transect of the NFP20-East line through the Central Alps 7

Figure 2.4 The Penninic nappes centred on the Adula-Cima Lunga nappe 11

Figure 2.5 Schematic paleogeographic setting of the mafic-ultramafic rocks from Cima di Gagnone and Alpe Arami 13

Figure 2.6 Schematic P-T-t diagram for the Cima Lunga unit 19

Chapter 3: Methods

Figure 3.1 Simplified geological map of the northern Cima Lunga unit at Cima di Gagnone showing sample locations 24

Figure 3.2 Simplified geological map of the Alpe Arami peridotite and eclogite locality 25

Figure 3.3 Generating Kikuchi bands using the ESBD technique 27

Figure 3.4 Schematic diagram showing the representation of rock sample fabric on a pole figure diagram 30

Figure 3.5 An example of stimulated omphacite LPO under simple and pure shear 31

Figure 3.6 Two types of deformation fabric in omphacite 32

Figure 3.7 Schematic figure showing the preferred orientation of an omphacite crystal to generate S-type fabric 33

Chapter 4: Map Structures and Microstructures

Figure 4.1 Equal area stereonet plots showing structural measurements from Cima di Gagnone 34

Figure 4.2 Geological map of the Cima Lunga unit at Cima di Gagnone with structural measurements 35
Figure 4.3 Structural map of the Cima Lunga unit at Cima di Gagnone showing traces of D2 axial planes 36
Figure 4.4 Interpretative structural cross-section of the northern Cima Lunga unit 38
Figure 4.5 The Claro syncline 39
Figure 4.6 Schematic diagram of the Claro syncline after D1 and D2 41
Figure 4.7 Representative photomicrographs of country rock lithologies from Cima di Gagnone 44
Figure 4.8 Series of photomicrographs showing progressive grain size reduction in the Simano orthogneiss 45
Figure 4.9 Field photo of eclogite sample SM12 46
Figure 4.10 Representative photomicrographs of eclogites and ultramafic-derived schists from Cima di Gagnone and Alpe Arami 47
Figure 4.11 Selected composition phase maps constructed with EDS data 48

Chapter 5: Textures

Figure 5.1 Pole figures showing omphacite LPO measured using the ESBD technique 52
Figure 5.2 Pole figures showing examples of poor LPO patterns of omphacite 54

List of Abbreviations

Mineral	Abbreviation
Albite	ab
Biotite	bt
Chlorite	chl
Diopside	di
Garnet	grt
K-feldspar	kfs
Kyanite	ky
Muscovite	ms
Olivine	ol
Omphacite	omp
Plagioclase	pl
Pyrope	prp
Quartz	qz
Rutile	rt
Staurolite	st
Talc	tlc
Tremolite	tr

Mineral abbreviations after Kretz,1983.

Term	Abbreviation
Foliation	S
Lineation	L
Fold	F
Fold axis	FA
Fold axial plane	FAP
Deformation stage	D
Pressure	P
Temperature	T
Time	t

Acknowledgements

First and foremost, I would like to thank my supervisor Dr. Djordje Grujic for giving me the opportunity to learn and explore the world of Alpine geology in Switzerland through a challenging but rewarding journey; for his timeless patience and creativity in teaching me to see geological structures in three-dimensions; for his support, encouragement, and inspiration throughout this learning and writing process. It was a pleasure to work with someone so intelligent and curious, always fascinated by the challenges ahead.

I would also like to thank Dr. Martin Gibling for his constructive feedback and continued guidance through the writing process. Also, I extend my gratitude towards the Department of Earth Sciences, for your company and mentorship during the years I've spent here.

Finally, I thank my family, friends, and loved ones for their generous support, motivation, and wonderful humour in making this an enjoyable final year. We did it!

Chapter 1: Introduction

Beginning in the early 1980s, successive discoveries of coesite, the high-pressure polymorph of silica, in the Western Alps and the Caledonides (Chopin, 1984; Smith, 1984) provoked interest and led to the greater understanding of ultrahigh-pressure (UHP) metamorphism. UHP metamorphism is established as eclogite-facies metamorphism that has occurred within the coesite stability field (>25-30 kbar, Fig. 1.1; Carswell & Zhang, 2000). Many subsequent discoveries and studies of UHP terranes have led researchers to examine processes involved in the subduction of crustal materials and their exhumation from previously unsuspected depths (>100 km).

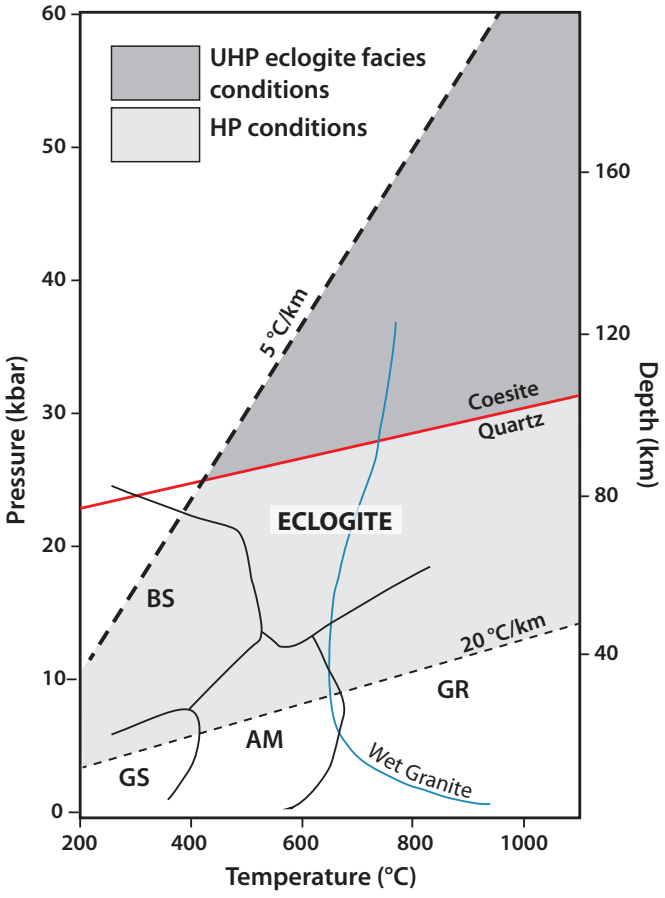

Figure 1.1. Simplified P-T facies diagram showing the P-T stability field for eclogite-facies ultrahigh-pressure metamorphism. The typical subduction zone and continental geothermal gradients are shown. GS: greenschist facies, BS: blueschist facies, AM: amphibolite facies, GR: granulite facies.

UHP terranes lie within major continental collision belts (Fig. 1.2) and share some common characteristics: UHP records are preserved mainly in volumetrically small mafic eclogites and garnet peridotites enclosed within host gneisses; they are of upper- to mid-crustal origin; and, exhumed UHP units are positioned between lower-grade metamorphic units and regionally near suture zones (Ernst et al., 2007).

We find this exact scenario in the (U)HP Adula nappe in the Penninic nappes of the Central Alps. Lying in the shadows of the great UHP coesite-bearing Dora-Maira massif (Western Alps; Chopin 1991), the Adula nappe has also experienced regional

(U)HP eclogite facies metamorphism despite the lack of evidence for coesite. The Adula nappe contains small horizons of eclogite and ultramafic rocks that record UHP metamorphism (Dale & Holland, 2003).

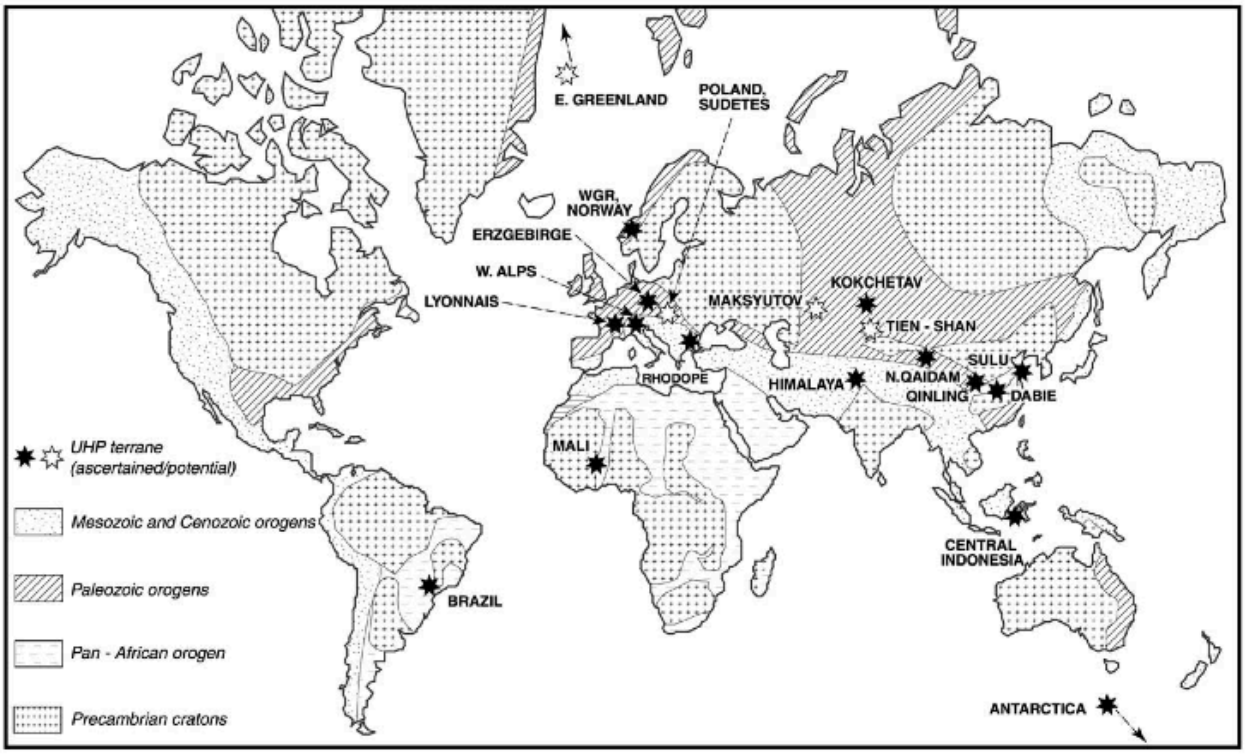

Figure 1.2. Global distribution of UHP metamorphic terranes. Figure from Chopin (2003).

To transport continental crust, without melting, to such extreme UHP depths and back is an impressive natural phenomenon. In the return process, as isothermal gradients (isotherms) relax, (U)HP rocks are subjected to heating and can be overprinted by lower metamorphic facies minerals. Presence of (U)HP rocks at the Earth's surface suggest that exhumation until mid-crustal levels (ca. greenschist facies conditions) was rapid. These UHP rocks carry a unique record of their metamorphism and exhumation, providing us with important insight into deep geodynamic processes that are otherwise difficult to image.

1.1 Scope of this study

The purpose of this study was to contribute to understanding how the (U)HP rocks in the Adula nappe were emplaced between adjacent lower-pressure country rocks. The main objective was to identify the kinematics of emplacement of (U)HP rocks through structural and textural analyses on the eclogite-facies rocks and their country rock gneisses. This was achieved through field and laboratory structural observations. Field methods involved mapping deformation structures and collecting oriented rock samples. Laboratory methods involved microstructural observations for sense of shear, while textural analyses for lattice preferred orientation in omphacite were performed on (U)HP rocks.

Earlier textural studies suggest that omphacite texture in eclogite rocks serve as a useful tool for examining deformation regimes active during (U)HP metamorphism (e.g. Bascou et al., 2002). We used this research approach on the (U)HP rocks of the southwestern Adula nappe (Cima Lunga unit at Cima di Gagnone) as they have not been thoroughly studied with this technique.

In this study, we report structural, textural, and petrographic observations of the study area along with a thorough literature review for the Central Alps. Unfortunately, the observed microstructures and textures were not suitable for a full kinematic investigation in the scope of this thesis. This was a first account of omphacite fabric at the Cima di Gagnone locality of Cima Lunga. Our observations did, however, enhance the current knowledge of the contrast between Cima Lunga unit and the main Adula nappe. When combined with earlier geochronological and textural data available in the literature, this study provides new insight to support the notion that the Cima Lunga unit can be considered as a separate lithotectonic unit from the main Adula nappe.

Chapter 2: Geological Background

2.1 Introduction to the Alpine Framework

The Alps are an active orogen resulting from the convergence of the European continent ("Europe") with the Adriatic plate ("Adria"; equivalent to present-day Africa) and closures of intervening oceanic basins (Fig. 2.1). The Alpine mountain chain extends from northern Corsica in the west to Vienna in the east. It is ca. 1200 km long and 150-250 km wide and is narrowest in the transect of Switzerland. Geographically, the Alps are commonly subdivided into three sections: the Western, Central, and Eastern Alps. The entire Alpine orogen has been subject to a wealth of studies over 150 years due to its complexity and undoubted natural beauty, which proves to be irresistible for the curious geologist. As such, a hindrance to providing an overview of Alpine geology is the intricate nomenclature for regional tectonic units that changes across nations. For clarity in the scope of this study, I will focus on the Central Alps in Switzerland using nomenclature common to this region.

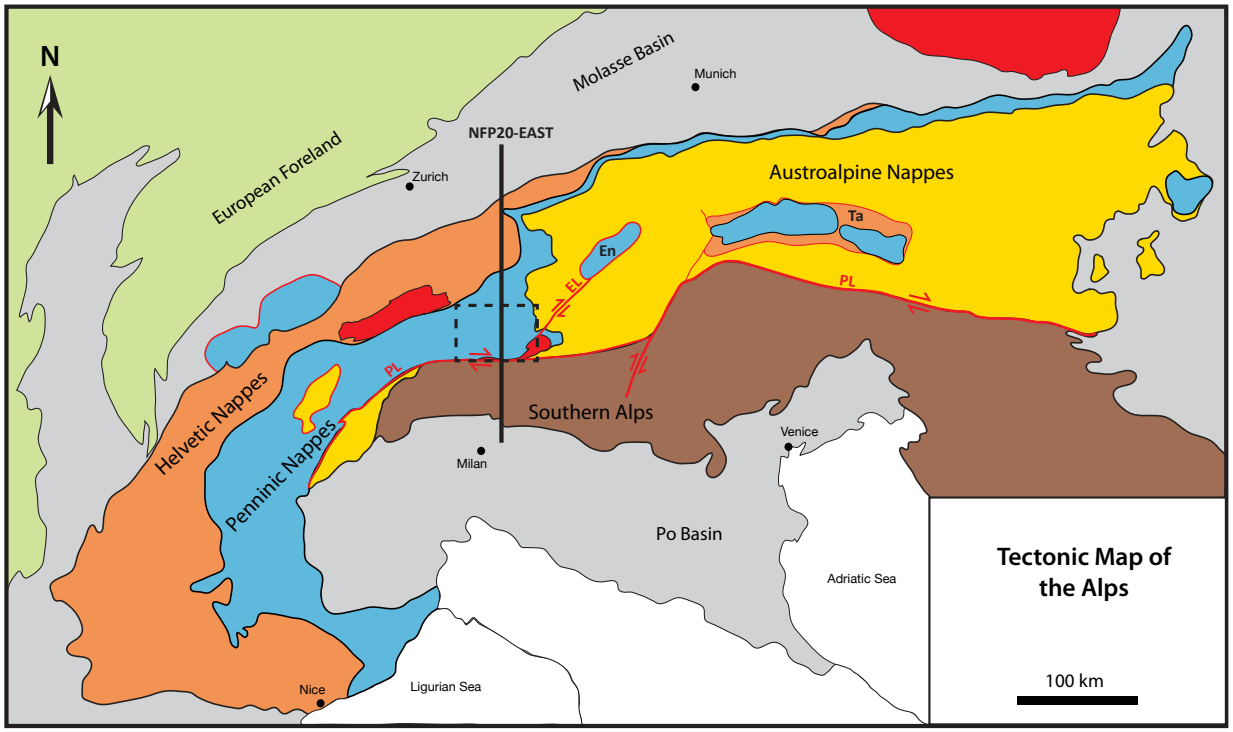

Figure 2.1. Simplified tectonic map of the Alpine system showing the major tectonostratigraphic units and lineaments of the Periadriatic line (PL). En: Engadine window; Ta: Tauern window. Dotted box shows the location of Fig. 2.4. Figure adapted from Pfiffner (2005) and Schmid et al. (1996).

The present day configuration of the Alps reflects its tectonic evolution through orogenic processes of subduction, collision, and collapse. Kinematic data based on magnetic isochrons in the Atlantic Ocean show convergence between Africa and Europe in the Cretaceous, 120-83 Ma (chrons M0 and 34; Rosenbaum et al., 2002). Periods of rapid convergence occurred in the Late Cretaceous and Eocene-Oligocene, with periods of relative quiescence in the Paleocene and Miocene (Rosenbaum et al., 2002).

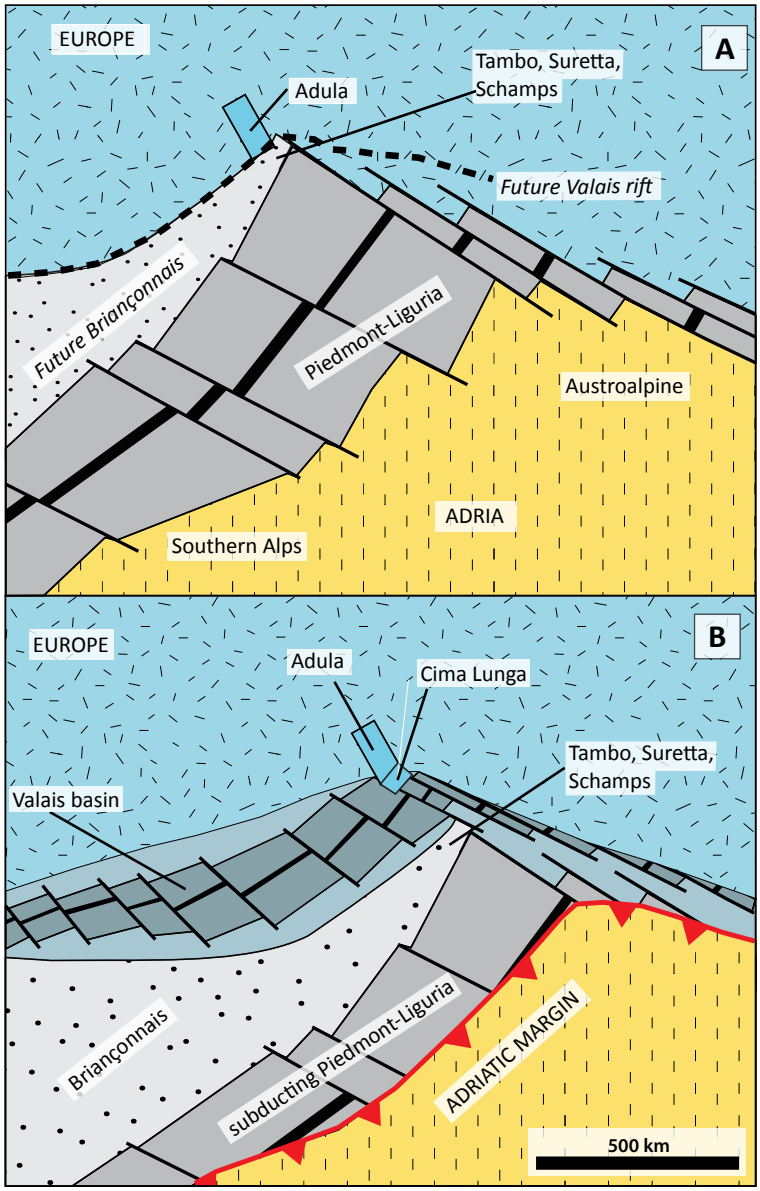

Figure 2.2. Paleogeography of the Central Alps. (A) Late-Jurassic to early Cretaceous. The Piedmont-Liguria ocean separates Europe from Adria. The future Adula nappe belongs to the European continental margin north of the Valais rift. (B) Early Cretaceous. Subduction of the Piedmont-Liguria ocean beneath Adria. The Briançonnais ribbon microcontinent and the Valais ocean will eventually follow into the subduction zone. Figure modified from Dale & Holland (2003).

A brief chronology of subduction and collision events began with formation of two oceanic basins, Piedmont-Liguria and Valais (jointly belonging to Alpine Tethys), kinematically linked to the opening of the north Atlantic Ocean. The Piedmont-Liguria ocean opened in the mid-Jurassic as an eastward extension of the Atlantic (Fig 2.2A; (Frisch, 1981; Schmid et al., 2004). The Valais ocean opened north of Piedmont-Liguria in early Cretaceous times and was separated from Piedmont-Liguria by Briançonnais, a ribbon microcontinent.

Contemporaneously, the Briançonnais drifted to the south, southward-directed subduction of Piedmont-Liguria basin beneath the Adriatic plate commenced (Fig. 2.2B), and led to the collision of Briançonnais and the Adriatic continental margin. This was the first phase of continent-continent collision in the Alps and occurred in the middle Cretaceous and was followed by a period of relative quiescence in the Paleocene (Frisch, 1981; Rosenbaum et al., 2002). In the second phase of continent-continent collision, Europe collided with Adria by the southward subduction of the Valais ocean and the European margin beneath the Adriatic margin during the Eocene (between 50 and 47 Ma; Schmid et al., 1996). Convergence has continued at a slower rate since the Early Miocene.

The comprehensive work by Schmid et al. (1996) integrated geologic data and results of two major seismic investigations, the Swiss National Research Project 20 (NFP20-East; Pffifner et al., 1990) and the European GeoTraverse (EGT), to image the deep structure of the Central Alps. These studies presented cross-sections through the Swiss-Italian Alps depicting all the major Alpine tectonic units (Fig. 2.3) and are essential in any discussion of Alpine geology.

2.1.1 Large Scale Structures and Units

The four major tectonostragraphic domains in the Alps are the Helvetic, Penninic, Austroalpine, and Southern Alpine units (Fig. 2.1, 2.3). Situated north of the Periadriatic Line, the first three domains are characterized by northward foreland-directed nappe complexes, whereas the Southern Alpine unit (Southern Alps), south of the Periadriatic Line, is characterized by a south-verging fold-and-thrust belt (Schmid et al., 2004). The Periadriatic Line, and related lineaments mark the southern limit of Alpine metamorphism (Fig. 2.1; Schmid et al., 1989).

A nappe is an allochthonous thrust sheet that has detached from its deeper substrate and moved along a shallowly dipping surface, i.e. a décollement or detachment surface (Twiss & Moores, 2007). A nappe can originate as a fold nappe or thrust nappe; fold nappes form when

the overturned limb of a large-scale recumbent fold becomes progressively sheared and thinned out by ductile deformation, whereas thrust nappes are bounded by a thrust at the base do not originate from a pre-existing fold.

The Central Alpine system was formed by northward thrusting and nappe stacking, which is now characterized by isoclinal, north-closing recumbent anticlines separated by pinched-in synclines containing the Mesozoic cover (Helvetic nappes) of the European basement (Penninic nappes). (Fig. 2.3; Maxelon & Mancktelow, 2005).

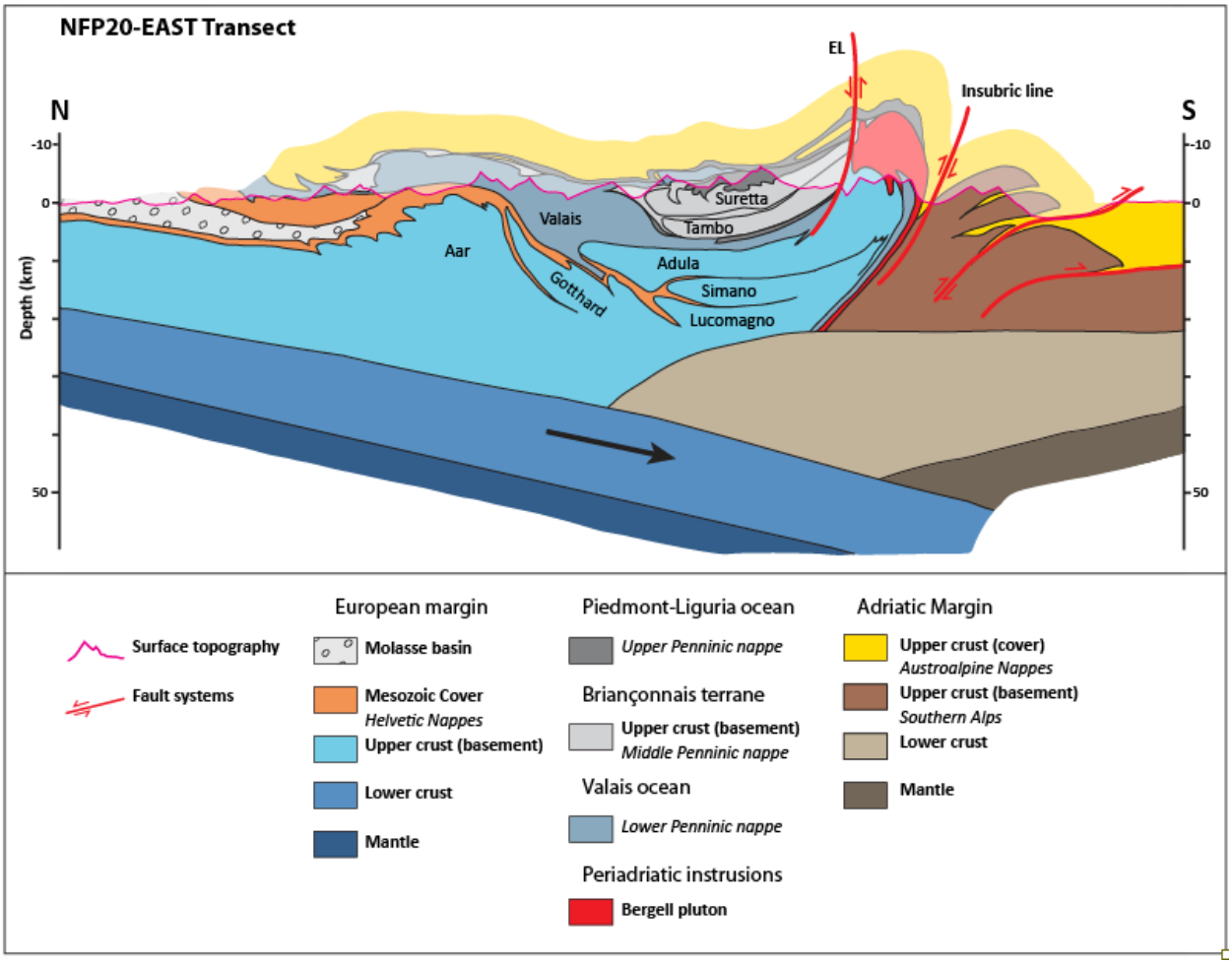

Figure 2.3. Schematic transect of the NFP20-East line through the Central Alps, after Schmid et al. (1996), and Schmid et al. (2004), as constrained by seismic reflection data. EL: Engadine line; Insubric line is the central segment of the Periadriatic line. The location of the transect is shown in Figure 1.1.

2.1.1.1 European Plate

Helvetic Nappes

The Helvetic nappes are limestone-dominated, Mesozoic to Paleogene cover sediments derived from proximal European margin deposits (Schmid et al., 2004). These are predominately allochthonous sediments that represent the most external units to the Central Alps (Fig. 2.1). The Helvetics are only preserved as thin slices in the foreland due to extensive erosion in the Paleocene (Pfiffner, 2000; Fig. 2.3). Prior to nappe emplacement, the rocks of the Helvetic nappes were the cover sediments of the Penninic nappes. These sediments have generally undergone anchizone to sub-greenschist facies metamorphism (Bousquet et al., 2008).

Penninic Nappes

The Penninic nappes are derived from various paleogeographic domains; they comprise oceanic sediments and lithosphere from two Mesozoic oceanic basins and European continental crust (Froitzheim, 2012). The Penninic nappes can be divided into four subsections as differentiated by their provenance (Table 2-1; Schmid et al., 2004). Valaisan and Helvetic Mesozoic sediments usually define the nappe boundaries of crystalline basement units. The overall Penninic nappe complex dips gently towards the north and describe a forward dipping-duplex geometry (Fig. 2.3). Near the northern and southern extremity, the nappes steepen to sub-vertical attitudes at the Northern Steep Belt (NSB) and the Southern Steep Belt (SSB), respectively.

Table 2-1

Subsection	Provenance of dominant lithology	
Upper Penninic	Piedmont-Liguria ocean sediments	
Middle Penninic	Briançonnais continental crust	
Lower Penninic	Valais ocean sediments	} collectively form the Lepontine dome (or Lepontine nappes)
Sub-Penninic	distal European continental crust and margin	

The Penninic nappes are well exposed in the Central Alps, but only appear as tectonic windows in the Eastern Alps (Tauern and Engadine windows; Fig. 2.1). The Penninic nappes record two stages of Tertiary Alpine metamorphism:blueschist to eclogite facies UHP metamorphism followed by low-pressure high-temperature metamorphism from greenschist to amphibolite facies metamorphism (Bousquet et al., 2008). The Lower and Sub-Penninic nappes form the Lepontine dome, a structural and metamorphic dome defined by dominant regional attitudes of foliation, lineation, and regional metamorphic mineral isograds (Merle et al., 1989). The Lepontine dome can be further divided into the Ticino subdome to the east (shown in the field of view of Fig. 2.4), and the Simplon subdome to the west. The Sub-Penninic nappe within the Lepontine dome contains the high- to ultrahigh pressure Adula nappe rocks pertinent to this study.

Adula Nappe

The Adula nappe is the structurally highest unit among the Sub-Penninic nappes and is located on the eastern flank of the Lepontine dome within the Ticino subdome. Beneath and west of it are the pre-Mesozoic granitoid and metapelitic gneisses and schists of the Simano and Lucomagno-Leventina nappes; above is the Misox zone containing units predominantly of Valais provenance (i.e. Lower Penninic nappe; Fig. 2.4).

2.1.1.2 Adria Plate

Austroalpine nappes

The Austroalpine nappes occupy the tectonically highest position in the Alpine nappe stack (Fig. 2.1, 2.3). They are derived from the northern Adriatic continental margin as allochthonous thrust sheets toward overriding the Penninic and Helvetic nappes. Eclogite facies metamorphism has only been recorded in lower basement units (e.g. Pohorje nappe; Koralpe and Saualpe massifs); most other parts of the Austroalpine nappes are non- to weakly-metamorphosed (Bousquet et al., 2008; Janák et al., 2004).

Southern Alps

The Southern Alpine nappes are derived from the more southerly continental crust of the Adriatic plate and do not record Alpine metamorphism (Bousquet et al., 2008).

2.2 Adula Nappe

The Adula nappe was paleogeographically located on the southernmost European margin (Fig. 2.2B; (Schmid et al., 1996). It is a structurally and lithologically heterogenous unit of pre-Mesozoic Variscan-deformed basement rocks (granitoid gneisses and metapelitic schists) with minor Alpine-metamorphosed Mesozoic continental margin sediments, eclogites, amphibolites, and ultramafic rocks (Pfiffner & Trommsdorff, 1998; Dale & Holland, 2003 and references therein). The southwestern portion of Adula is the Cima Lunga unit that contains the study localities Cima di Gagnone and Alpe Arami (Fig. 2.4). The Adula-Cima Lunga nappe is regarded as the only unit in the Central Alps that bears (U)HP Alpine-metamorphosed rocks (Bousquet et al., 2008). These next sections will introduce the field area and summarize the petrographic, metamorphic, and structural record of the Adula-Cima Lunga units.

2.2.1 Field Area

The study areas are Cima di Gagnone and Alpe Arami, located in the Cima Lunga unit of the Adula nappe (Fig. 2.1). These localities host (U)HP eclogite-bearing rocks with pressure conditions that have not been discovered elsewhere in adjacent nappes. Two additional samples were collected in the main body of the Adula, near the San Bernadino pass, about 30 km northeast of Cima di Gagnone. The Cima di Gagnone area is located between Swiss coordinates 707’500–709’500/130’500–132’500, and Alpe Arami is around 719’000–121’000.

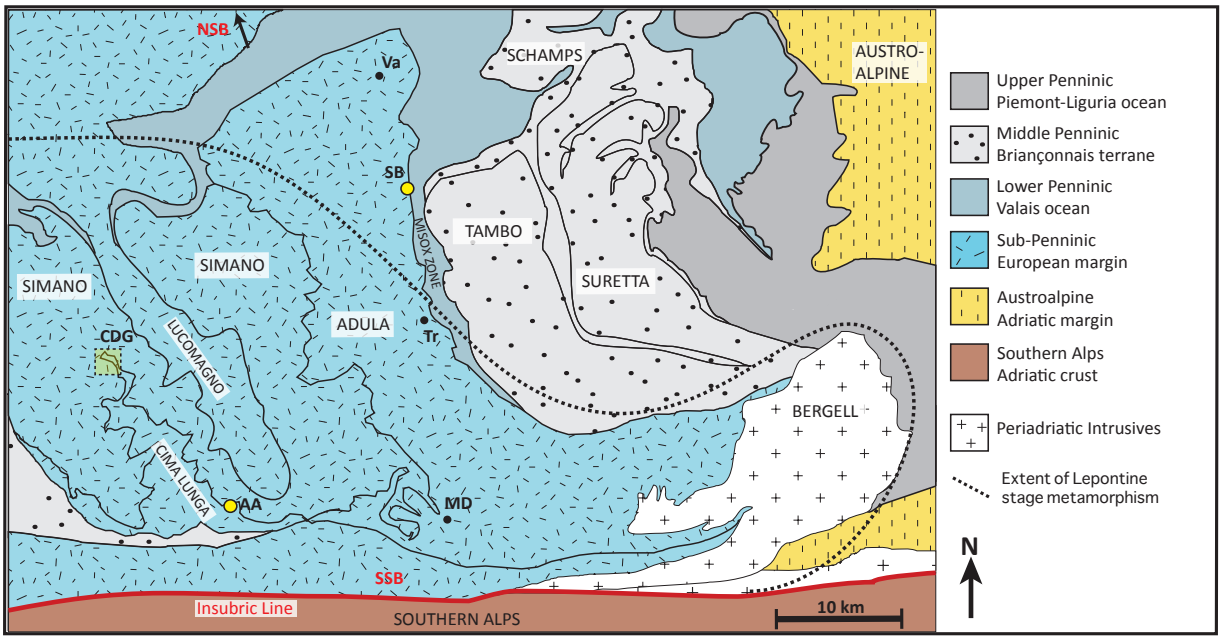

Figure 2.4. The Penninic nappes centred on the Adula-Cima Lunga nappe. Lithotectonic units are grouped by paleogeographic affinity. Map area is indicated in Fig. 2.2 and shows the approximate location of the Ticino subdome of the Lepontine Dome region. The field areas are highlighted as CDG: Cima di Gagnone; AA: Alpe Arami; SB: San Bernadino. Other localities, Va: Vals; Tr: Trescolmen; MD: Mont Duria. Figure modified from Dale & Holland (2003).

2.2.2 Petrography

The Adula nappe complex consists of ortho- and paragneisses of the European basement with metapelites, metamafics, and carbonaceous metasediments. The higher part of the Adula contains basements rocks intercalated with calcareous sediments, which are associated with ultramafic and mafic (U)HP rocks (Pfiffner & Trommsdorff, 1998). Ultramafic lenses and boudins are increasingly more abundant in the southern Adula, such as the Cima Lunga unit where ultramafic lenses are on the meter to kilometre scale (Pfiffner & Trommsdorff, 1998). These ultramafic rocks (mantle-derived garnet peridotite, enstatite-olivine-chlorite and talc-chlorite rocks) accompany metamafics (eclogites and amphibolites), and metacarbonate rocks (ophiocarbonates), all of which are volumetrically small in comparison to the country rock gneisses.

Whereas the country rock gneisses are derived from continental Europe, the origin of the protoliths to the Adula mafic-ultramafic rock suite requires more discussion. First, in the Cima Lunga portion of the Adula, the mafic and ultramafic rocks are ascribed to MORB- flows and dykes, and the lithospheric mantle, respectively (Evans et al., 1981; Evans et al., 1979; Pfiffner & Trommsdorff, 1998). Evans et al. (1981) proposed a shallow crustal origin for the protolith of the mafic rocks based on analyses of trace element data, which indicated a low-pressure MORB-type origin, similar to tholeiites of Mid-Atlantic Ridge basalts. Petrological evidence suggested a lithospheric mantle origin for the ultramafic rocks; they were partially exhumed during rifting of the Valais ocean and was later intruded by MORB- flows and dykes at ocean floor levels (Fig. 2.5). This shallow level would allow for the observed rodingites at Cima di Gagnone (CDG), which are closely associated with serpentinization of ultramafic rocks (Trommsdorff et al., 2000). Rodingites are metasomatic rocks that develop adjacent to mafic and within ultramafic rocks undergoing serpenitization (Rice, 1983). The lack of rodingites at Alpe Arami suggests that its lithospheric mantle protolith was not entirely exhumed to oceanic levels prior to Alpine-related subduction (Trommsdorff et al., 2000). The Alpe Arami rocks must have been derived from *subcontinental* lithospheric mantle, adjacent to the CDG derivatives (Fig. 2.5).

In summary, the Cima Lunga mafic-ultramafic rock suite were derived from lithospheric mantle and MORB-type rocks at shallow oceanic crustal levels, which were then subjected to eclogite-facies metamorphism during Alpine subduction beneath the Adriatic plate. This ocean floor containing the mafic-ultramafic and carbonaceous protoliths to the Alpine UHP rocks likely represents the Valais ocean, and we should expect Mesozoic sediment ages for any Valais-derived rocks.

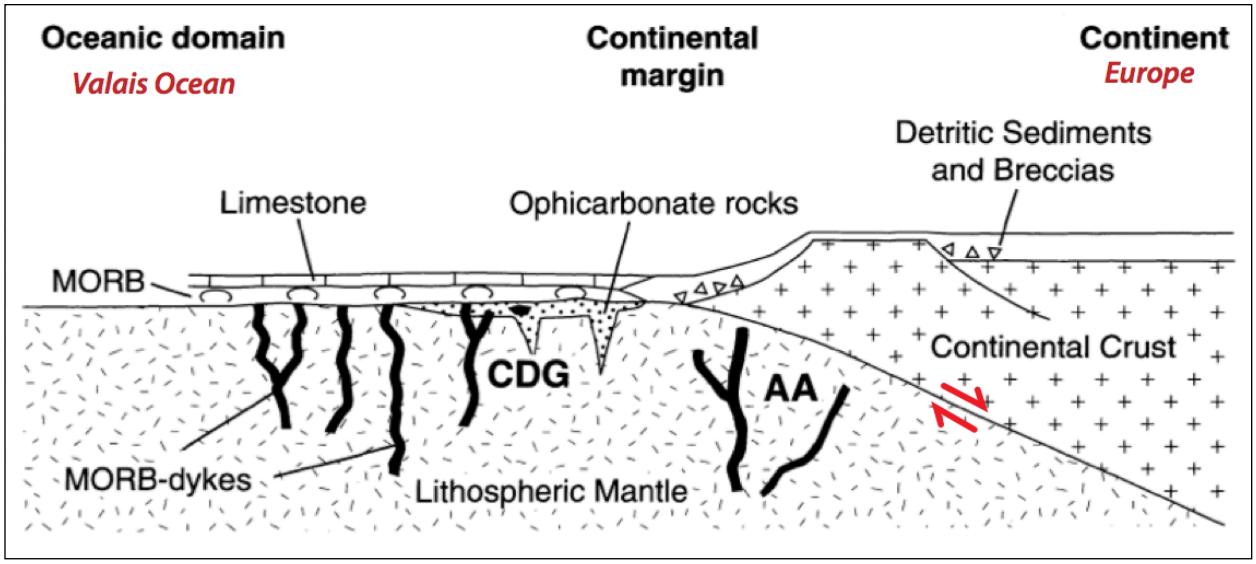

Figure 2.5. Schematic drawing showing the paleogeographic setting of the mafic-ultramafic rocks of Cima di Gagnone (CDG) and Alpe Arami (AA). The mafic rocks correspond to MORB- flows and dykes, whereas ultramafic rocks are derived from an exhumed and partly exhumed lithospheric mantle, in the case of CDG and AA, respectively. Figure from Trommsdorff (2000).

2.2.3 Deformation History

The deformation history of the Adula nappe cannot be explained independently without considering the entire Penninic nappe pile of the Lepontine dome. Numerous structural studies (e.g. Merle et al., 1989; Maxelon & Mancktelow 2005 and references therein) have shown that the Lepontine region underwent several deformation stages. However, not all identified deformation stages are pervasive throughout the entire Lepontine region, nor do the absolute chronology of stages coincide between individual studies.

Since the structural observations of this study only cover a small areal (<10 km^2), it is difficult to relate and establish larger-scale deformation stages. Instead, a chronology of deformation stages (D_x) correlating structural observations from several previous studies are presented. Five designated deformation stages D_0-D_4 will be used in the remainder of this study (Table 2-2).

The first stage D_0 encompasses all deformation attributable to pre-Alpine (e.g. Varisican orogeny) and early Alpine activity leading up to UHP conditions in the Eocene. The D_0 stage is associated with convergence and subduction of the European margin beneath the Adriatic plate. Any preserved D_0 fabric is restricted to mafic and ultramafic boudins (Grond et al., 1995); their orientation does not bear kinematic significance because the boudins have rotated by overprinting of Alpine deformation .

D1 describes deformation under post-peak pressure conditions during isothermal decompression associated with nappe stacking, folding and thrusting. The D_1 stage accommodated the greatest amount of strain as high P-T conditions (eclogite to amphibolite facies) allowed for ductile deformation.

D2 describes deformation under high temperature (amphibolite facies) conditions that is associated with the Lepontine dome formation (e.g. Merle et al., 1989). The refolding of D_1 structures created Type 2 and 3 fold interference patterns (Ramsay & Huber, 1987). Fold axial planes (FAP_2) of isoclinal recumbent folds dipping NNW denote a pervasive regional axial planar foliation, that is sub-horizontal but variable in dip-direction due to gentle perturbations along the regional-scale (FAP_3) fold axes.

Stages D_3-D_4 are attributed to developing two subdomes, the Northern and Southern Steep Belts, and their associated fabrics under greenschist facies conditions. $D_{3,4}$ occurred during a stage of rapid cooling where backfolding and backthrusting were prominent along the SSB and NSB.

Table 2-2. Deformation stages in the Lepontine region, where possible, only stages affecting the Adula nappe are considered.

Nomenclature used for this study

Deformation Stage	D_0	D_1 High Pressure	D_2 High Temperature	D_3	D_4
Main Structures	Magmatic layering, mineral lineation, preserved in mafic and ultramafic boudins	Regional isoclinal folding FA1 ~ N-S; stretching lineation L1 ~ N-S; S1 dipping gently NW	Strong isoclinal recumbent folding FAP2 ~ NNW, stretching lineation L2 ~ N-S // FA2	Refolding and steepening of D2 fabrics along the SSB; localized steep FAP and stretch L3 // FA3	Localized folding at NSB and SSB, FA4 ~ NE-SW; local crenulation fabric
Tectonic Setting	Pre-Alpine to onset of peak-pressure conditions	Post-peak pressure; nappe stacking, isothermal decompression	Reheating event; refolding D1 structures atHT forms regionally pervasive fabric	Rapid cooling; exhumation aided by backfolding and backthrusting; continued Lepontine dome formation	
Kinematics	–	Top to N	Top to SSE; top to N near the frontal NSB	Near horizontal top to W	–
Time	Pre-Tertiary to Early Eocene?	~40-32 Ma	35-30 Ma	32-25 Ma	<25 Ma
P-T (Barrovian) Conditions	Blueschist to Eclogite facies	Amphibolite facies	Amphibolite facies	Greenschist facies	Greenschist facies

Previous works

Merle et al., 1989 and references therein	–	–	HTD	RD, Insubric phase	Insubric phase
Maxelon & Mancktelow 2005	Pre-Alpine	D1	D2	D3	D4
Grond et al., 1995	Pre-D1	D1	D2		D3, D4
Pfiffner & Trommsdorff 1998	D0	D_{HP}, D1	D2	D3	D4
Nagel 2008 and references therein	–	Zapport	Leis/Claro	Leis/Cressim	Carassino
Nagel 2002a	–	D1	D2	D3	–

2.2.4 Metamorphic Conditions and Geochronological Data

The majority of researchers consider the Adula nappe as having experienced a single Alpine (U)HP metamorphic event corresponding to Paleocene-Eocene subduction and collision (e.g. (Froitzheim et al., 1996; Nagel et al., 2002b). However, in light of recent evidence for Variscan-age (U)HP metamorphism preserved in eclogitic and orthogneissic Adula rocks (Herwartz et al., 2011; Liati et al., 2009), the scenario of a single (U)HP event becomes a matter of debate; this will be addressed later in this study.

High pressure rocks throughout the Adula nappe show a common Alpine metamorphic evolution with clockwise P-T paths and an apparent pressure and temperature field gradient from north to south (Dale & Holland, 2003). P-T paths show prograde metamorphism from blueschist to eclogite facies conditions and generally isothermal decompression to amphibolite and greenschist facies. The Adula nappe also experienced a heating event during its decompression (Bousquet et al., 2008). The result is a bimodal P-T path showing distinct pressure and temperature peaks, where peak-pressure assemblages are overprinted by a later thermal peak: the Lepontine HT event (Fig. 2.5; Merle et al., 1989).

The present-day metamorphic field gradient in the eclogitic and ultramafic rocks of Adula nappe shows an apparent southward increase of peak temperature conditions and a southwestward increase of peak pressure conditions (Dale & Holland, 2003). There is also an increasing degree of post-HP amphibolite facies overprint from north to south, corresponding to the late orogenic Lepontine thermal event (Nagel, 2008).

High pressure conditions

High- to ultrahigh-pressure metamorphism is preserved in eclogites, garnet amphibolites, garnet peridotites, and metapelites (Nagel, 2008). In the northern and central Adula, peak pressure conditions are 12 kbar (Vals) and 22 kbar (Trescolmen) at 500-650 °C (localities shown in Fig.

2.4); for the southern Adula, peak pressures are 25 kbar at 780 °C, as derived from eclogite rocks (Dale & Holland, 2005). Further south at Alpe Arami and Mont Duria, UHP conditions are obtained from garnet peridotites where peak-pressure conditions range from 30 kbar at 850 °C (Nimis & Trommsdorff, 2001), up to 59 kbar at 1180 °C based on various independent thermobarometers (Paquin & Altherr, 2001). At Cima di Gagnone, peak pressure reached 30-35 kbar (Becker, 1993).

The timing of peak pressure events are constrained by various geochronological methods. Sm-Nd dating of garnet peridotites and eclogites at Alpe Arami yield consistent garnet-clinopyroxene whole rock isochron ages of 44-40 Ma; these are interpreted to be cooling ages that represent the timing of eclogite facies metamorphism (Becker, 1993). Similarly, U-Pb zircon ages within garnet pyroxenites and eclogites yield ages of 43 ± 2 Ma, interpreted to represent the timing of eclogite facies metamorphism; and garnet peridotites yield ages of 35.4 ± 0.5 Ma that are interpreted as timing of HP-decompression melting of peridotites (Gebauer, 1996). In terms of the ultramafic rock association, the 43 Ma may be related to prograde metamorphism and incipient melting during the initial subduction. At Gorduno, 4 km southeast of Alpe Arami (see inset map of Fig. 3.2), eclogite Lu-Hf ages yield 38.1 ± 2.9 Ma to approximate timing of peak-pressure conditions; at Alpe Repiano, 5 km southeast of Cima di Gagnone, partially retrogressed eclogites yield Lu-Hf ages of >47.5 Ma (Brouwer et al., 2005)

High temperature conditions

The general observation of a high-temperature (HT) stage occurring after the peak pressure stage holds true for the P-T evolution of the lower and sub-Penninic nappes (Bousquet et al., 2008). The metamorphic isograds post-date nappe formation since isograds cross-cut nappe boundaries. Nagel et al. (2002a) mapped four staurolite mineral zone boundaries in the Adula and observed a southward-increase of peak temperatures during isothermal decompression. Established isotherms and isobars based on studies of amphibolite facies metapelites (i.e. highest temperature metamorphic assemblages equilibrated during the main thermal peak)

show a continuous increase in temperature from 500 °C in the north to >650 °C in the south, with overall thermal equilibration pressures of 5.5 kbar (Dale & Holland, 2003). In the southernmost part of the Lepontine Dome, the SSB rocks have undergone Tertiary migmatization (Burri et al. 2005). Thermobarometric conditions of partial melting estimated from amphibole-bearing leucosomes are 6-8 kbar and 700 ± 50 °C. The northern Adula reached peak temperature conditions at 35-38 Ma during its subduction; the southern and central Adula reached peak temperature conditions between 28 Ma and 20 Ma, respectively (Engi et al., 1995 as cited in Dale & Holland, 2003). Gebauer (1996) indicates that migmatization occurred at 32.4 Ma while Burri et al. (2005) indicate that the migmatization event occurred between 25 and 30 Ma.

P-T-t Path

Mineral zone boundaries, thermobarometric isograds, and retrogressive amphibolite facies conditions are continuous and cross-cut through nappe boundaries. Since 33 Ma, the mafic-ultramafic rocks and country rock gneisses have experienced a common metamorphic history (Gebauer, 1996). This 33 Ma age was documented in metamorphic zircon domains of mafic-ultramafic rocks and in magmatic domains of leucocratic gneisses; this age represents granulite facies passage for Cima Lunga rocks implying that eclogite facies conditions must have occurred prior to 33 Ma (Gebauer, 1996).

In the Cima Lunga unit, the P-T path to peak pressure, decompression, and late reheating occurred within 20 Ma (Gebauer, 1996); the P-T-t-d path for the mafic-ultramafic rocks and the country rock gneisses in Figure 2.6 summarizes the metamorphic conditions with respect to deformation stages presented in this Chapter.

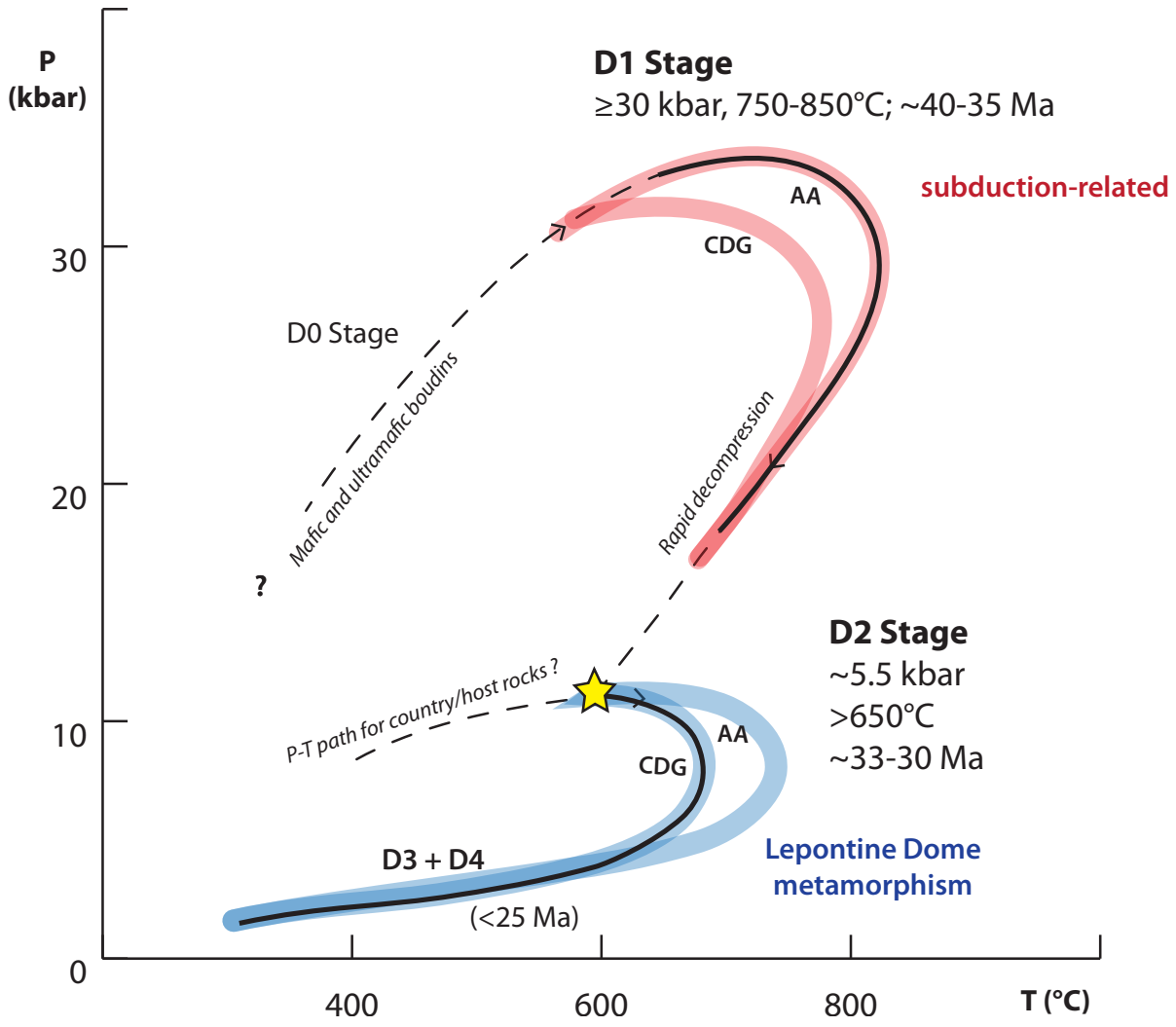

Figure 2.6. Schematic P-T-t diagram for the Cima Lunga unit; P-T conditions are constrained by various thermobarometric methods as described in text. It is likely that are two separate paths for the mafic - ultramafic rocks and the lower-pressure country rocks. The (U)HP/HT conditions are associated with subduction, whereas the later reheating event is associated with the Lepontine dome formation. The yellow star marks when the mafic-ultramafic rocks and the country rocks experienced the same metamorphic history, at 33 Ma.

2.3 Unresolved Geological Problems

Tracing the P-T-t path for the Adula-Cima Lunga nappe

Since (U)HP mineral assemblages are not found in the country rock gneisses, this leads to the question of whether the gneisses experienced the same (U)HP conditions as the mafic-ultramafic rocks. Several petrologists suggested that the Adula nappe was assembled in the

subduction channel as a melange after peak-pressure conditions (Trommsdorff 1990, as cited in Nagel 2008). This idea has henceforth been challenged by pre-Alpine HP metamorphic ages recorded in an eclogite rock of the central Adula (Herwartz et al., 2011).

Geochronological and geochemical data from two recent studies have shown evidence for a pre-Alpine HP metamorphic event preserved in the northern and central Adula nappe, exclusive of the Cima Lunga unit. The first study by Liati et al. (2009) used zircon U-Pb SHRIMP dating and REE geochemistry of zircons from eclogites and country rock gneisses; they concluded the following:

1. The northern and central Adula was affected by a pre-Alpine HP metamorphic event, at 330-340 Ma and 370 Ma, respectively.
2. Protolith ages of orthogneisses and eclogites are Ordovician and Proterozoic, respectively; and maximum sedimentation ages of paragneisses are Cambrian-Ordovician.
3. Metamorphic zircon domains record a 33-32 Ma Alpine event, interpreted to represent a HT event (Lepontine metamorphism).
4. No geochronological evidence was found for the Late Eocene UHP metamorphism.

The northern and central Adula appears to have experienced a Variscan HP metamorphic event. Both the Variscan eclogite rocks and country rock gneisses were metamorphosed to HP-HT conditions as a coherent (or in situ) unit because both rocks were folded together during the early stages of Alpine deformation (D1 and D2), and show the same metamorphic ages (Liati et al., 2009).

In contrast, the Cima Lunga unit record 35 Ma HP metamorphic zircon age (Gebauer, 1996), 37.5 Ma Sm-Nd mineral ages (Becker, 1993), and ~38 Ma Lu-Hf mineral ages (Brouweret al., 2005), all of which were not found or correlated to in the Adula. In addition, no Variscan sedimentation ages have been recorded in Cima Lunga paragneisses. Based on these lines of evidence, Liati et al. (2009) suggest that the Adula nappe consists of different tectonic slices

(i.e. a *lithospheric mélange* by Trommsdorff 1990) metamorphosed at different times. This supports the interpretation of the Adula-Cima Lunga unit and in particular the Southern Steep belt, as a “tectonic accretion channel” (Engi et al., 2001).

A recent study by Herwartz et al. (2011) used the Lu-Hf isochron method in garnets of eclogite rocks from the central Adula (at Trescolmen, Fig. 2.5) and found two distinct populations of HP garnets at 333 Ma and 38 Ma in one sample. Therefore, the Adula eclogites must have been subducted to mantle depths during both the Variscan and the Alpine orogeny. After the initial Variscan subduction, the eclogite was exhumed and incorporated into continental crust. Later, during the Alpine orogeny, this eclogite-bearing continental rock segment (i.e. the Adula) was subducted and exhumed as a coherent unit to and from the mantle (Herwartz et al., 2011).

Although Liati et al. (2009) and Herwartz et al. (2011) both present insight into the origin of mafic-ultramafic (U)HP rocks, they provide contrasting tectonic interpretations of the Adula body during subduction and exhumation in the Alpine orogenic cycle.

2.3.1 Motivation for Study

We can see that numerous studies over the past few decades were dedicated to investigate the complex geodynamic history of the Adula nappe. Although the petrography has been well-established, there are still unresolved discussions over the kinematics of emplacement and its timing with respect to the Alpine P-T-t path. To follow up on the idea of a “tectonic accretion channel” (Engi et al., 2001), we investigate the kinematics of (U)HP rocks in the Cima Lunga unit at Cima di Gagnone in search of evidence for simple shear through optical microscopy and a textural analysis. Published microstructural and textural studies conducted at Alpe Arami and throughout the Adula body show evidence for dominant pure shear deformation, but varying from transitional flattening to constriction (Bascou et al., 2001; Kurz et al., 2004). However, previous structural studies did not examine the microstructures and textures with respect to the

regional D1 and D2 structures. This is important for the accurate structural localization of the samples with respect to the nappe boundaries and within a subduction zone prior to nappe stacking and intense refolding that obscures initial geometries.

Because these are located at the base of the nappe, we expect that the UHP rocks of Cima Lunga unit at Cima di Gagnone and Alpe Arami to have clearer exhumation textures than those belonging to the rest of the Adula-Cima Lunga nappe because the protoliths Cima Lunga (U)HP rocks are Mesozoic in age, and thus, should have experienced less structural overprint relative to the older Paleozoic rocks of the main Adula nappe. Our texture results should help contribute to the discussion of whether the Cima Lunga unit and rest of the Adula nappe have experienced a common geodynamic history, and the structural relationship between the UHP rocks (>30 kbar) to the HP rocks of the main Adula (17-24 kbar).

Chapter 3: Methods

3.1 Field Methods

Field work was conducted during 16–23 September 2013 in the Cima di Gagnone and Alpe Arami region (Ticino, southern Switzerland). Both areas are in the Cima Lunga portion of the Adula nappe (Fig. 2.2). The lithological map from Grond et al. (1995) served as the main base map for field work at Cima di Gagnone (Fig. 3.1), complimented by the Swiss topographic map (No. 1293 “Osogna”, 1:25 000). The locations of all samples and structural measurements were recorded with a Garmin e-Trex device on the GNSS global positioning system, WGS84 projection. A simple lithological map by Moeckel (1969) was used as a base map for Alpe Arami (Fig. 3.2)

The primary objective of field work was to make structural observations and collect oriented hand samples of eclogites and host gneisses. Samples were collected for both microstructural and textural analysis in this study and for geochronology in a concomitant study. For each sample, the reference foliation, lineation, and orientation were noted. We collected 31 samples that can be broadly categorized into country rock ortho- and paragneisses and eclogite and associated mafic-ultramafic rocks. The majority of our eclogite samples were collected from a 400 m long mafic-ultramafic body enveloped within a paragneiss host; other eclogites were collected from small boudins along the north face of Cima di Gagnone (Fig. 3.1). Country rock samples were collected at the boundary between the Simano and Cima Lunga unit, and around any of the sampled eclogite-containing boudins. Two eclogite samples were collected from Alpe Arami (Fig. 3.2).

The second objective of field work was to locate and map large-scale folds since the detailed lithological map by Grond et al. (1995) lacks structural data. These structural measurements are

plotted to to define the traces of axial planes. Structural measurements will provide a reference frame to interpret the textural data.

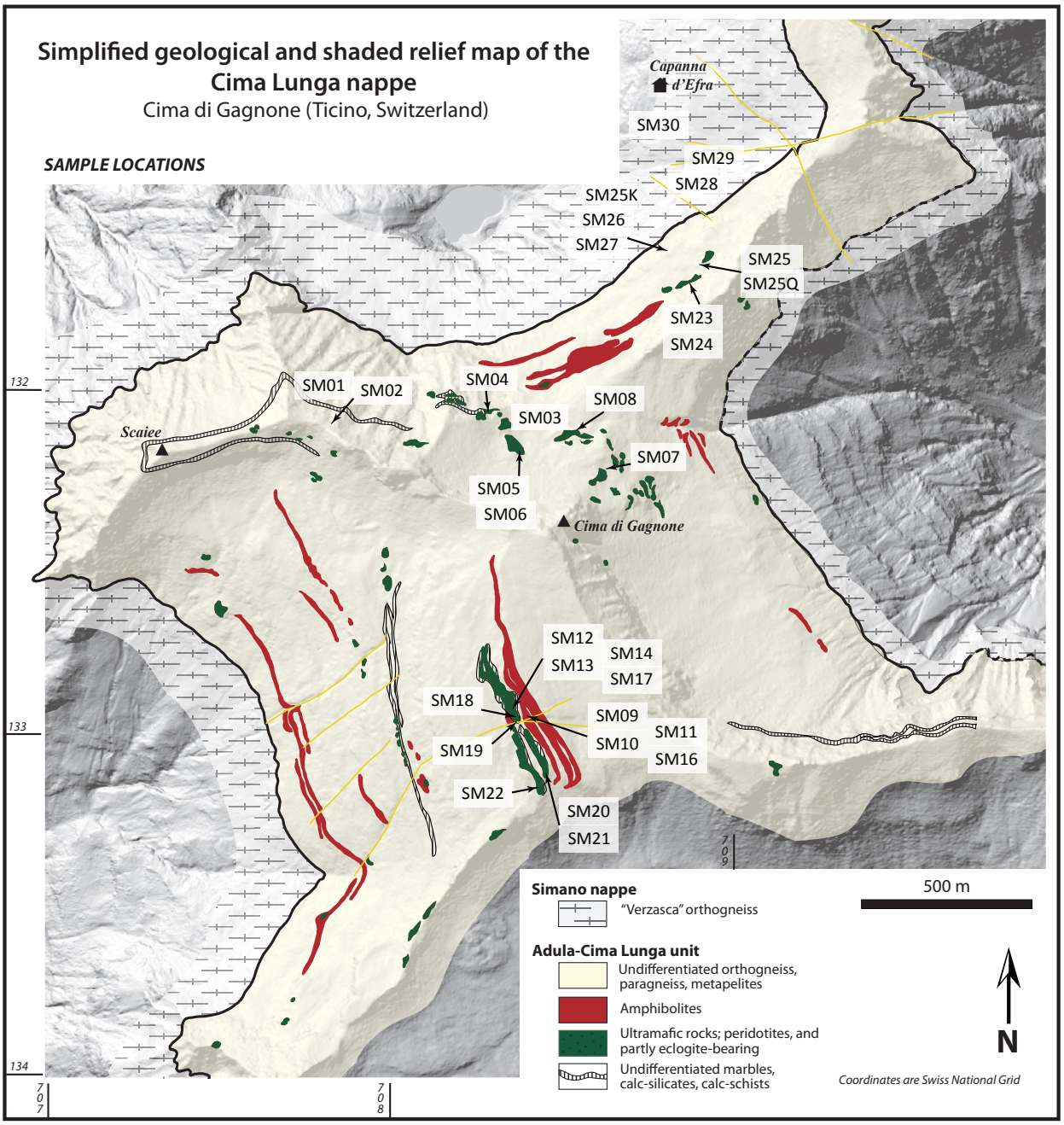

Figure 3.1. Simplified geological map of the northern extent of the Cima Lunga unit showing sample locations. The geological map is overlain on top of a DEM to enhance the appearance of these near-horizontal units in mountainous terrain. Lithological units are drawn from Grond et al. (1995); the DEM map was obtained from Swiss Federal Office of Topography. Location of this field area is marked in Fig. 2.5.

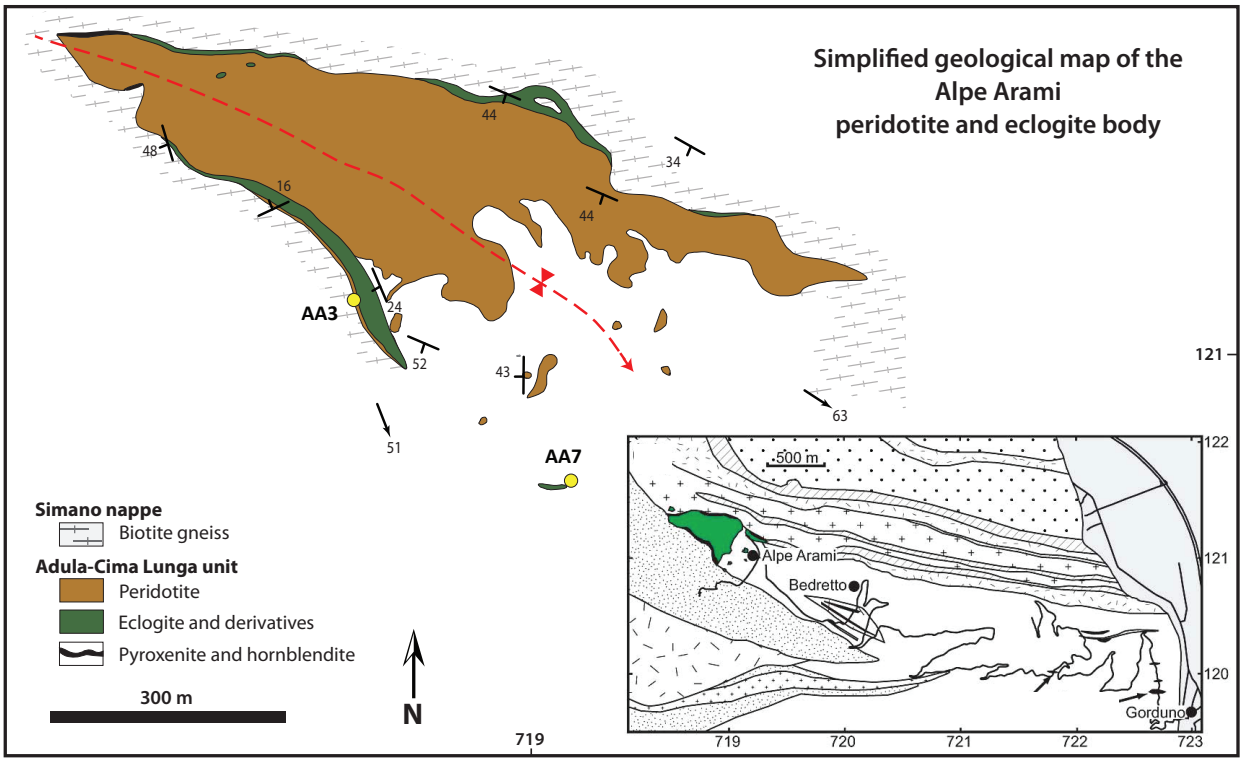

Figure 3.2. Simplified geological map of the Alpe Arami peridotite and eclogite locality in the Cima Lunga unit. Yellow dots show the locations of the two samples relevant to this study. Representative structural measurements from a previous field season are plotted (Grujic, pers. comm.). Lithological units are drawn from Möckel (1969); the inset map shows the approximate location of this body, which is marked in the regional map in Fig. 2.5. Coordinates are in Swiss National Grid.

3.2 Optical Microscopy

Petrographic observation of the microstructures of a rock in thin section is necessary to qualitatively examine the kinematics and regime of deformation. This method is intended to supplement the more quantitative textural analyses. For this study, standard covered thin sections were cut from hand samples and oriented perpendicular to macroscopic foliation and parallel to lineation, which was assumed to be the finite stretching lineation. Thin sections were prepared at Dalhousie University, and a Leica DMRX petrographic microscope was used to examine microstructures.

3.3 Electron Back-scatter Diffraction

The standard technique for textural analyses involves the electron back-scatter diffraction (EBSD) method. This is the preferred high-resolution method to determine the lattice (or crystallographic) preferred orientation (LPO or CPO) of minerals (Passchier & Trouw, 2005). Numerous studies (e.g. Mauler, 2000; Neufeld, 2008; Bascou et al., 2001) have confirmed the efficacy of ESBD for examining texture in eclogite rocks, since there is a strong relationship between deformation geometry and the LPO of omphacite, an eclogite facies mineral. We applied the ESBD technique to all eclogite samples because any resulting textures will correspond to D1 or (U)HP conditions. I will return to a detailed discussion of omphacite deformation fabric and LPO (Ch. 3.4) after an introduction to the ESBD methodology in the following section.

EBSD is a detection mode using a scanning electron microscope (SEM). Accelerated electrons from the primary beam are backscattered and diffracted by the lattice planes in the crystal structure. The intensity of the backscattered electrons (BSE) is controlled by the atomic weight of the material, which differentiates the phases present based on their mean atomic weight, and diffraction across the crystal lattice (*hkl)*. Orientation of the crystallographic planes and their *d*-spacing (distance between lattice planes) will affect the EBSD, producing bands of variable intensity, called Kikuchi bands or electron back-scattered patterns (EBSP; Fig. 3.3B).

An EBSD detector comprises a phosphor screen, which captures the Kikuchi bands, and a high-resolution camera that digitizes the pattern (Fig. 3.3A). The Kikuchi bands project the geometry of lattice planes in a crystal since individual bands and their intersections correspond to specific crystallographic planes and axes. Mineral grains and their orientations can be identified by their unique ESBP, which are automatically indexed and compared to a database of crystallographic structure information. The SEM maps the entire or part of the sample at a pre-determined step

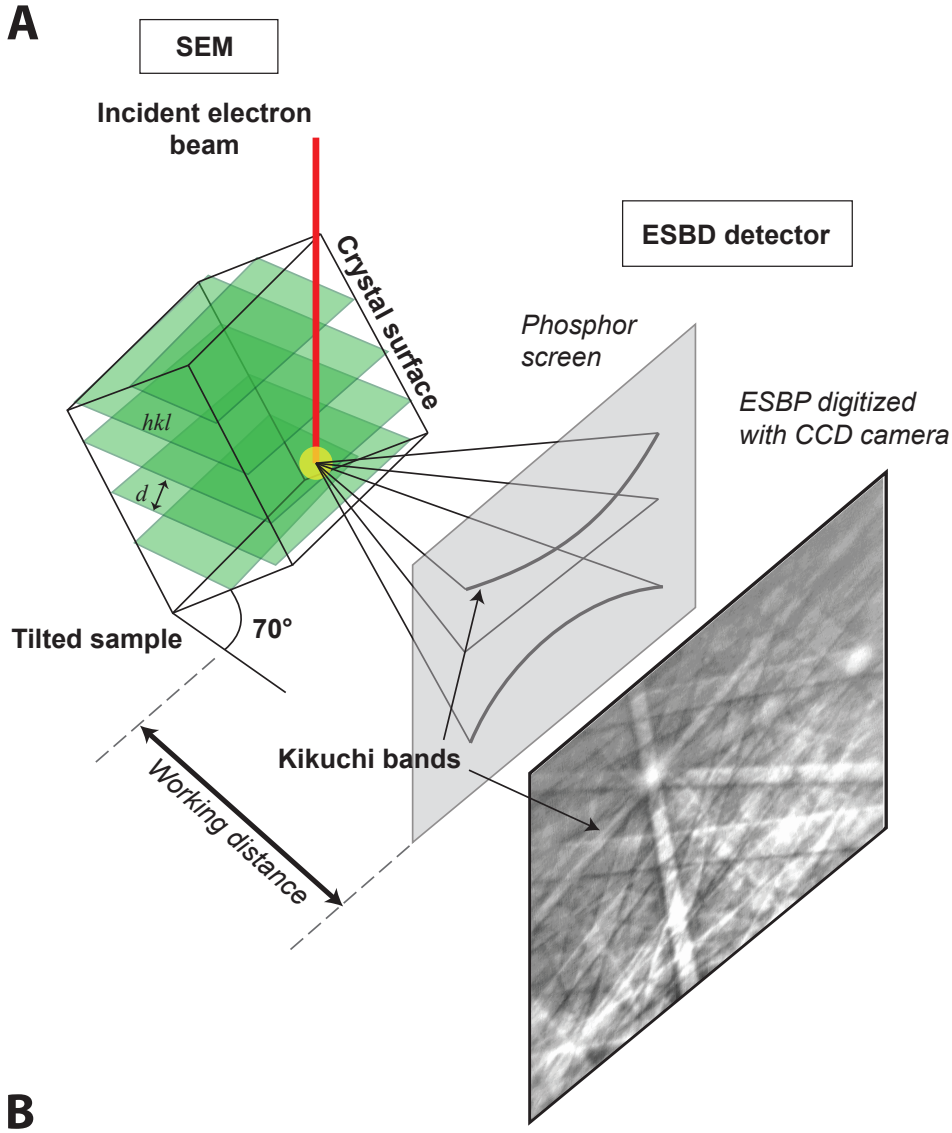

Figure 3.3. Generating Kikuchi bands using the ESBD technique.
(A) Schematic showing the configuration of the sample relative to the SEM beam and the formation of Kikuchi bands from BSE in the ESBD detector.
(B) Kikuchi bands generated from omphacite electron backscatter pattern. Orange lines represent the strongest indexing bands.

size, which defines the spatial resolution of the measurements. The automated scan of a sample produces a raster image of a defined resolution.

The LPO is obtained for each spot on the sample surface and can be displayed and adjusted in ESBD post-processing software. Since the LPO data are recorded with respect to the microscope stage, samples may need to be readjusted depending on its thin section orientation with respect to the microscope stage. This is to ensure that the projected LPO data properly reflect the kinematic plane of the thin section, which was intentionally referenced to macroscopic structures.

3.3.1 Sample Preparation

Eclogitic and mafic-ultramafic samples are cut such that they are parallel to lineation. If lineation is not well defined or ambiguous, samples are cut down-dip and perpendicular to foliation. This yields a thin section surface that is parallel to the principal kinematic plane for planar and linear fabric. Since ESBD analyzes the intensity of diffraction on the crystal surface, “superpolished” thin sections are used to minimize surface topography from damage during mechanical abrasion (Passchier & Trouw, 2005). The samples were mechanically polished with a fine diamond paste at Dalhousie University, and then polished using a 50 nm colloidal SiO_2 suspension on a vibratory polisher at the University of California, Santa Barbara.

3.3.2 Instrumentation

For this study, the ESBD analyses were performed using an HKL Technology Nordlys II ESBD detector mounted on a Quanta 400F MK2 scanning electron microscope at the University of California, Santa Barbara. This SEM also had an integrated energy dispersive X-ray spectroscopy (EDS) system that simultaneously collected chemical composition data with EBSD analyses. Operating conditions include a 15 mm working distance, 20 kV accelerating voltage,

and ca. 5 nA beam current with the samples tilted 70° from the beam normal (Seward, pers. comm.).

A total of 16 thin sections were mapped at 40 μm grid spacing. Although the SEM-ESBD system was capable of high-resolution mapping at 1 μm, our lower-than-ideal spatial resolution of 40 μm per pixel was chosen due to the time limitations of this study. For example, mapping the area of a standard thin section at 40 μm takes about 10 hours to complete.

I used the Channel 5 EBSD software from HKL Instruments to generate LPO pole figures and to readjust the orientations of any improperly cut samples.

3.4 Lattice Preferred Orientation

Lattice preferred orientation is a systematic arrangement of the crystal lattice for a specific mineral within a deformed rock (Passchier & Trouw, 2005). LPO develops as a result of plastic deformation. The type of LPO pattern is dependent on the slip systems that are operating and the amount of activity on each system (Passchier & Trouw, 2005). A slip system denotes a crystallographic plane and a direction within that plane where dislocation motion, or slip, occurs. The type of slip system active in a crystal depends on the critical resolved shear stress, which is a function of temperature and rheology. When a slip system is activated during deformation, the preferred orientation of the slip direction and the slip plane coincides with the flow direction and the flow plane, respectively (Nicolas & Poirier, 1976). Consequently, the LPO pattern obtained from a specific mineral can be used to interpret both the kinematics (i.e. flow regime) and temperature of deformation.

Pole Figures

LPO data are presented in pole figures, conventionally with lower hemisphere equal area projection, and in the structural X, Y, and Z reference frame. The Y-direction of the finite strain is

vertical and the X- and Z-directions run along the E-W and N-S pole figure axes, respectively (Fig. 3.4). In reference to the macroscopic fabric, poles to foliation (XY plane) is represented along Z, and lineation is the X-axis. An defined LPO pattern shows an array of concentrated poles and axes that can form girdles or point maxima perpendicular, parallel, or oblique to X or Z, depending on the deformation regime. LPO patterns are defined based on a specific mineral of interest.

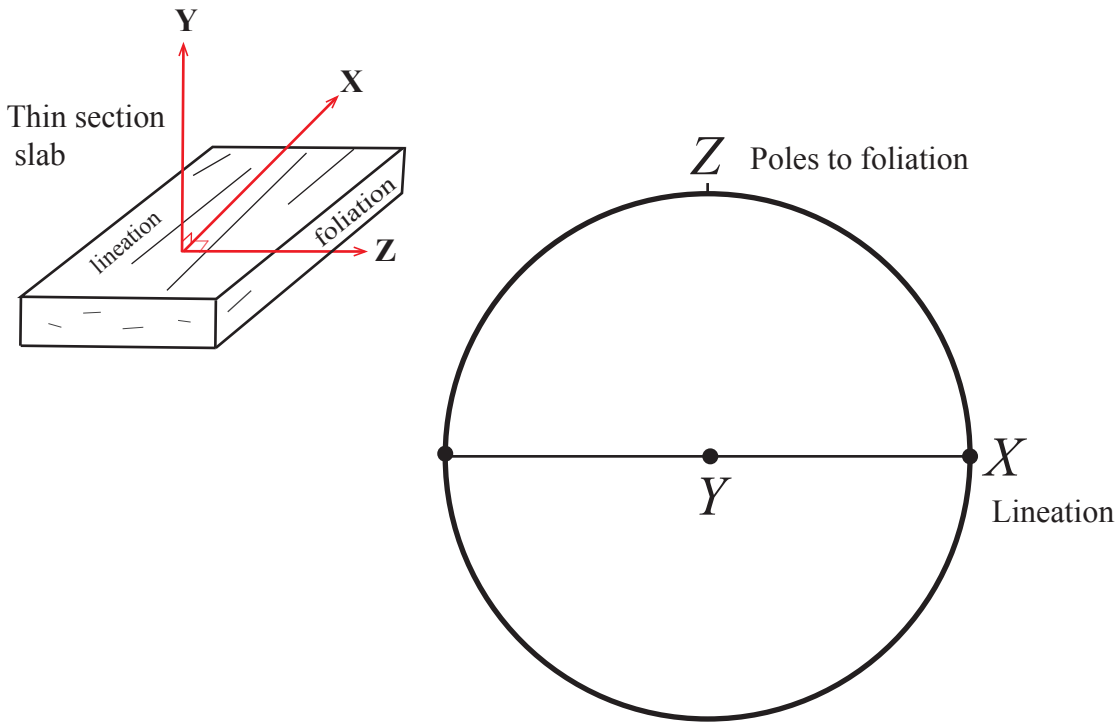

Figure 3.4. Schematic diagram showing the orientation of the rock sample fabric with respect to structural axes X, Y, Z and its representation in a pole figure diagram.

In pole figures, kinematic information can be deduced from the orientation of slip systems with respect to the structural frame. LPOs that are symmetrical (orthorhombic or rhombohedral crystal symmetry) with respect to foliation and lineation develop from coaxial deformation histories, whereas asymmetrical (monoclinic crystal symmetry) LPOs can develop from both

non-coaxial and coaxial deformation histories (Fig. 3.5). Note that the asymmetry in pole figures is referenced to the shear plane which lies at a low angle to the X (lineation) direction.
The main constituent minerals of eclogite rocks are garnet and omphacite. Several studies indicated that garnet rarely develops LPO due to its crystallography, and mostly behaves as a rigid body during ductile deformation (e.g. Godard & van Roermund, 1995 and references therein). Omphacite, however, has been documented as a suitable textural indicator for deformation (Neufeld et al., 2008, Godard & van Roermund, 1995). Since omphacite is an eclogite facies mineral, its texture will record deformation under eclogite facies conditions, and can be used to unravel tectonic processes active during (ultra-)high pressure events.

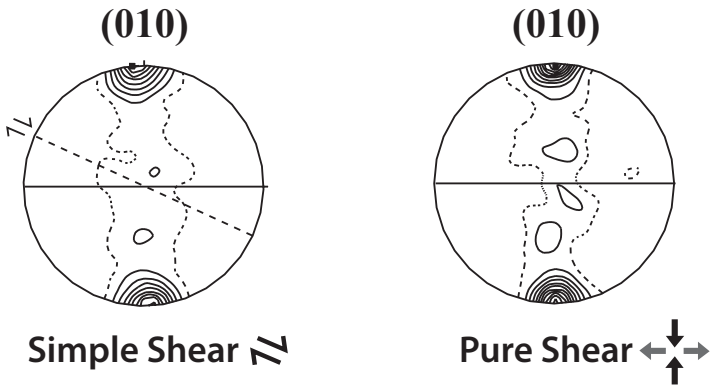

Figure 3.5. An example of omphacite LPO stimulated in a model with imposed simple shear and pure shear. The dotted straight line marks the shear plane and the direction of shear is horizontal to this plane. Figure from Bascou et al. (2002).

3.4.1 Omphacite LPO

Deformation Fabric

Omphacite LPO can be generated during ductile deformation in eclogite facies conditions. Omphacite has two principal types of deformation fabrics (Figure 3.6; Helmstaedt et al., 1972). The L-type or constrictional fabric is characterized by a concentration of [001]-axes parallel to the lineation, while (010)-poles form a girdle perpendicular to the lineation. The S-type or flattening fabric shows a concentration of (010)-poles normal to the foliation, while [001]-axes form a girdle corresponding to the foliation plane. An intermediate SL-type fabric shows transitional S- and L-type fabric features. The developed LPO fabric indicates the type of strain

from flattening to constriction, both for coaxial and non-coaxial deformation. (Godard & van Roermund, 1995; Helmstaedt et al., 1972).

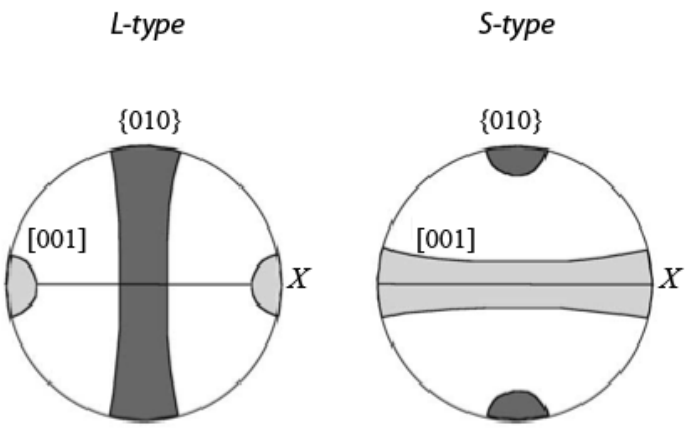

Figure 3.6. Two types of deformation fabric in omphacite. Dark grey represents the pattern exhibited by the (010) planes and light grey represents the orientation of the [001]-axes. Figure modified from Brenker et al. (2002).

Deformational regimes

Omphacite texture development was modelled under various strain regimes: simple shear, pure shear, axial compression, transpression, and transtension (viscoplastic self-consistent model by Bascou et al., 2002; Zhang et al., 2006). Modelled LPO patterns are indistinguishable from those of natural omphacite.

Omphacite LPOs show L-type fabric under simple and pure shear; but simple shear develops asymmetric patterns relative to the shear plane. In axial compression, LPOs develop S-type fabric that is symmetrical relative to foliation; the (010)-poles are strongly concentrated close to shortening direction perpendicular to foliation. In transpression, LPOs are similar to axial compression, but are oblique to foliation. LPOs developed under transtension are similar to those of simple shear, but are highly oblique to the shear plane and direction.

Slip systems and conditions

Several slip systems have been identified in omphacite through empirical studies. Omphacite LPO develop by dislocation glide on the [001]{110}, [001](100), 1/2<110>{110}, [100](010), and [001](010) slip systems (Bascou et al., 2002; Ulrich & Mainprice, 2005; Zhang et al., 2006). The notation of slip systems, for example [001](100), translates to slip in the [001] direction on the (100) lattice plane.

The two slip systems that are consistently discussed in literature are the [001]{110} and [001](100) systems. Slip on the {110} plays a major role in the orientation of (010)-poles perpendicular to foliation creating S-type LPO fabric (Fig. 3.7). The [001]{110} slip system is dominant in clinopyroxenes (omphacite and diopside) under moderate to high-temperature deformation (Bascou et al., 2002). The [001](100) system is active at low to moderate temperatures (Zhang et al., 2006).

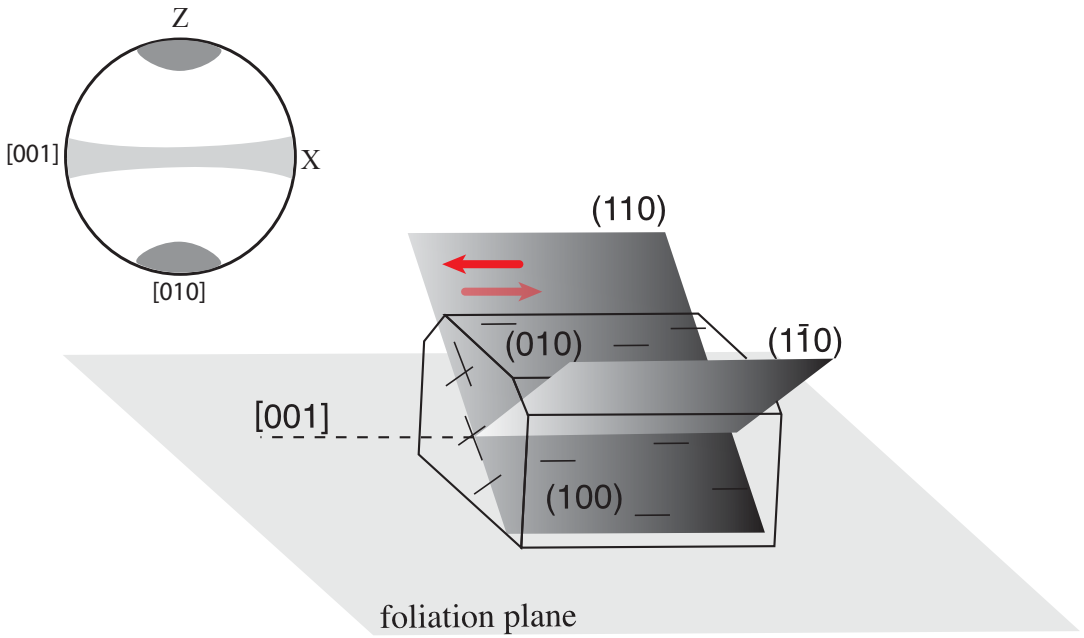

Figure 3.7. Schematic figure showing the preferred orientation of an omphacite crystal such that slip occurs on the {110} system to generate a S-type LPO fabric under simple and pure shear conditions. Figure modified from Bascou et al. (2002).

Chapter 4: Map Structures and Microstructures

Field observations and structural measurements enhance our interpretation of eclogite and ultramafic rocks and their association with country rocks at the base of the Cima Lunga unit. it was crucial to locate the eclogite samples with respect to the map-scale structures since the Penninic nappes have endured a complex multistage deformation history. This allowed for the proper interpretation of any microstructures with respect to the initial nappe boundaries.

4.1 Map-scale Structures

4.1.1 Field Observations

Our field observations and structural mapping focused on the pervasive D2 stage structures; these are presented on a simplified lithological map modified from Grond et al. (1995) (Fig. 4.2). Structural measurements are concordant with published data: the statistical fold hinge from Grond et al. (1996) is 160-07. Similarly, our observations show this NNW-SSE trend of lineations, while poles to foliations scatter around a great circle with its pole in the orientation of lineation and D2 hinges (Fig. 4.1). In addition, parallelism between F2 fold hinges and stretching lineations indicate concomitant NNW-SSE stretching. Guided by the cross-sections presented in Grond et al. (1995), and own field observations, we have drawn the traces of axial surfaces of D2 folds (i.e. FAP_2; Fig. 4.6).

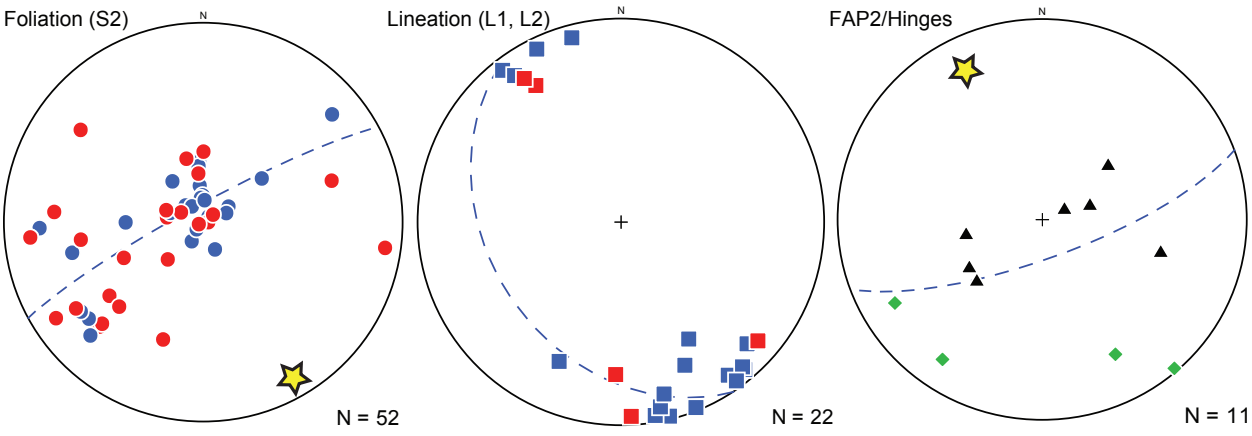

Figure 4.1. (Previous page) Equal area stereonet plots of structural measurements from Cima di Gagnone. Red points represent measurements taken within mafic or ultramafic units, whereas blue points are those from country rock gneisses. Axial planes: black triangles; hinges: green diamonds. Star shows the statistical fold axis. Blue great circle shows average plane.

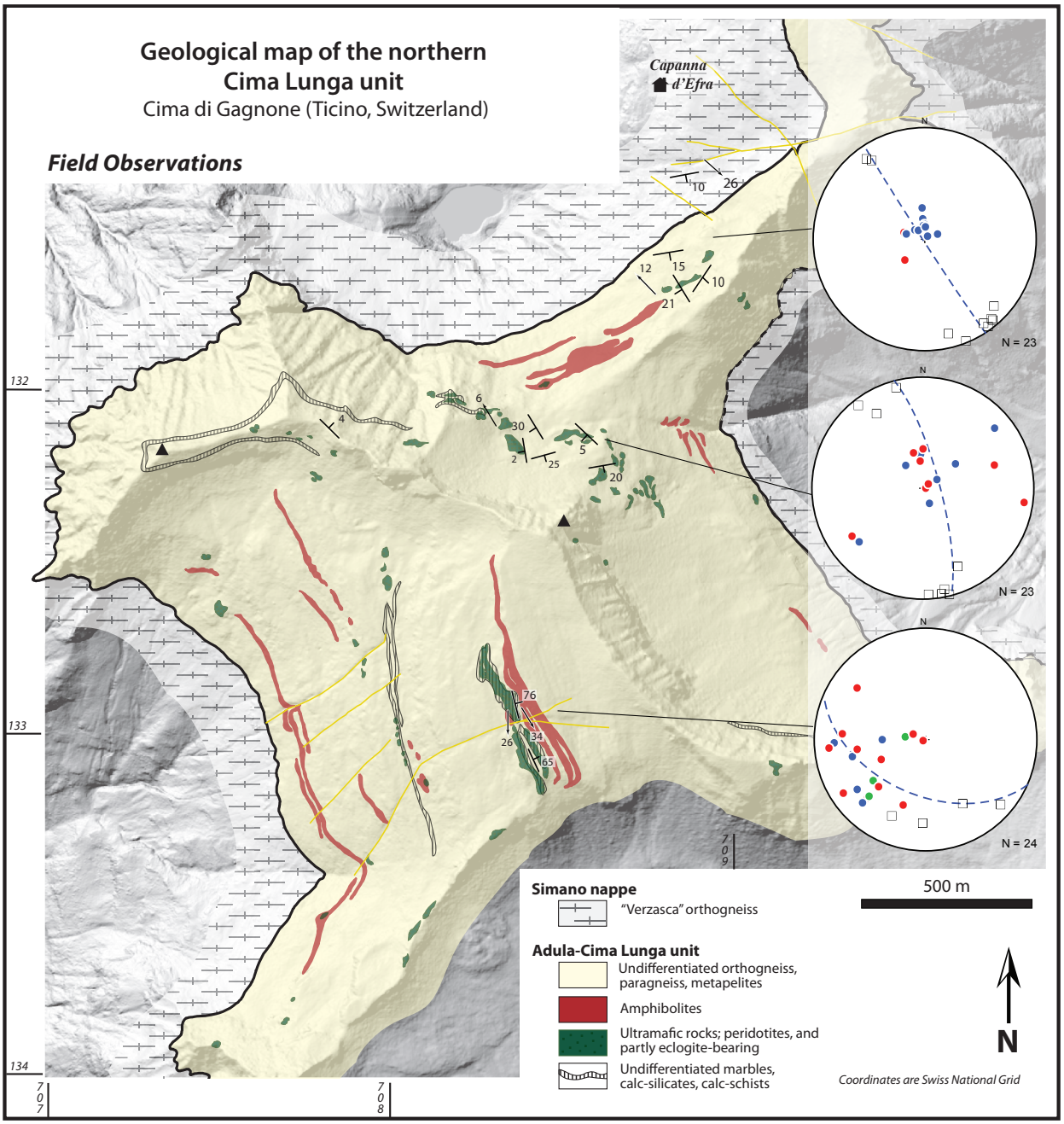

Figure 4.2. Geological map of the Cima Lunga unit at Cima di Gagnone showing structural measurements. Lithological units are drawn from Grond et al. (1995). Legend for stereographic projections: red points are mafic-ultramafic foliations, blue points are country-rock foliations, green points are eclogite layering; hollow squares are undifferentiated lineation measurements.

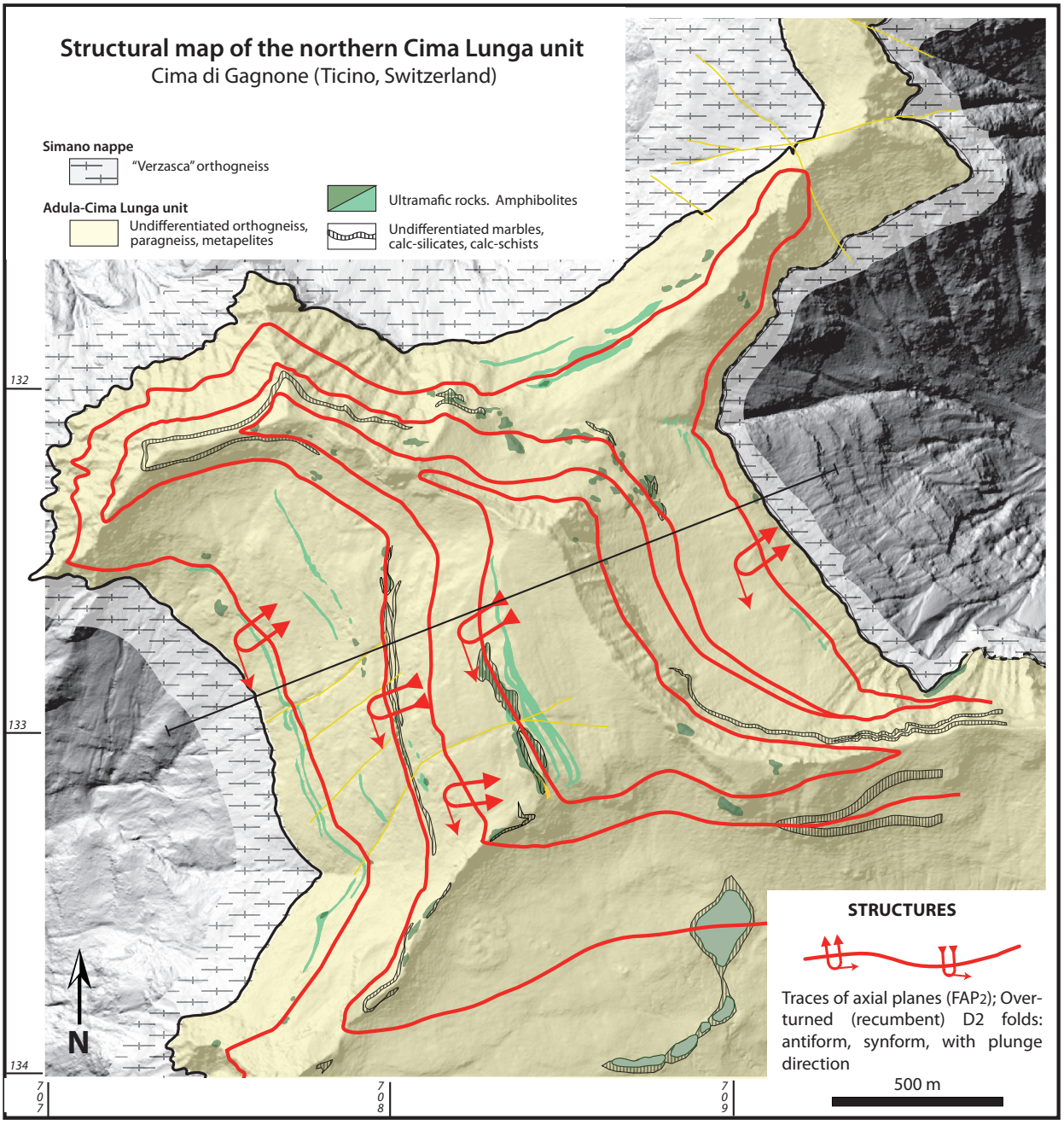

Figure 4.3. Structural map of the Cima Lunga unit at Cima di Gagnone showing traces of axial planes of D2 folds. Fold hinges are striking 160° from Grond et al. (1995).

Our field observations indicate that the D1 lineation in boudins are oblique to the D2 lineation, but these were not apparent in the stereonet plots, perhaps due to a small sample size (Fig. 4.1). However, previous structural mapping in the region (e.g. Grujic & Mancktelow 1995; Maxelon & Mancktelow 2005; Rütti et al., 2005), have shown that the fold hinges of the two folding stages (F1 and F2) were initially at a high angle to each other.

4.1.2 Discussion

The Cima di Gagnone area is folded into a series of isoclinal, west-closing recumbent folds (Grond et al., 1995). Based on the redrawn Cima di Gagnone map with traces of axial surfaces (FAP2), two structural interpretations can be made:

- Most boudins of mafic-ultramafic rocks belong to the same “stratigraphic” horizon, while the remaining boudins are situated on another horizon (Fig. 4.4A). These two horizons are the two limbs of an F1 folds as suggested by Grond et al. (1995).
- The alternate interpretation is where almost all mafic, ultramafic rocks, marbles and calc-silicates belong to the same horizon interpreted as tightly flattened and boudinaged F1 synform (Fig. 4.4B).

In both cases we interpret the discontinuous layer(s) of mafic-ultramafic rocks as the main F1 structure separating the Variscan basement units of Simano beneath from Adula above. Meanwhile, all the mafic-ultramafic rocks and associated marbles and calc-silicates belong to the core of a south-closing recumbent syncline, the Claro syncline (Fig. 4.5; Maxelon & Mancktelow, 2005). According the to the first interpretation, the first phase fold is tight to isoclinal. Although Grond et al. (1995) suggest the F1 and F2 hinges are coaxial, the map pattern and the cross section suggest otherwise, i.e., a Type 2 fold interference pattern in which both initial fold hinges and axial surfaces are folded. In Figure 4.3A, the F1 fold hinge goes in and out of the cross-section plane at the top and bottom end of the F1 axial trace; the fold closes south. Prediction of this structural solution is that the metapelites in the core of the Claro

syncline should have Mesozoic depositional ages. According to the second interpretation (Fig. 4.6B), the cores of the F2 synforms (east- and south-closing recumbent folds) contain the Simano basement while cores of antiform (west- and north- closing recumbent folds) contain the Adula basement. Both interpretations change the position of the Simano–Cima Lunga nappe contact, effectively adding “slices” of the Simano unit within the Cima Lunga unit.

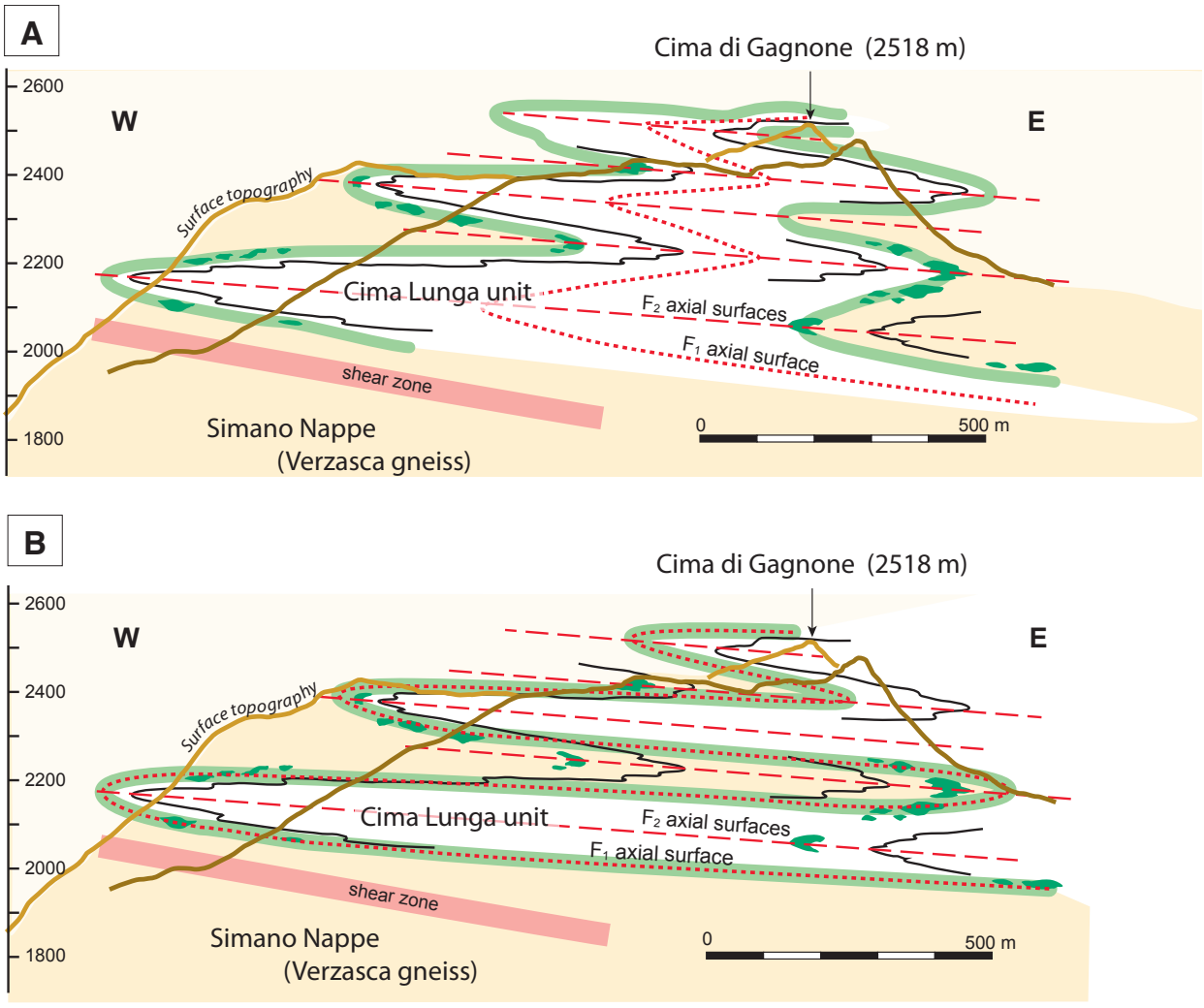

Figure 4.4. Interpretative structural cross-section of the northern Cima Lunga unit. Figure modified from Pfiffner and Trommsdorff (1998). (A) Locations of ultramafic boudins are projected and are interpreted to belong to the limbs of a south-closing recumbent F1 fold (Claro syncline). This interpretation changes the nappe contact between the Simano (pale yellow) and Cima Lunga (white) units. (B) Locations of ultramafic boudins are projected and are interpreted to belong to *a tightly flattened and boudinaged horizon* of the F1 fold (Claro syncline). Note the position of the F1 axial surface compared to (A).

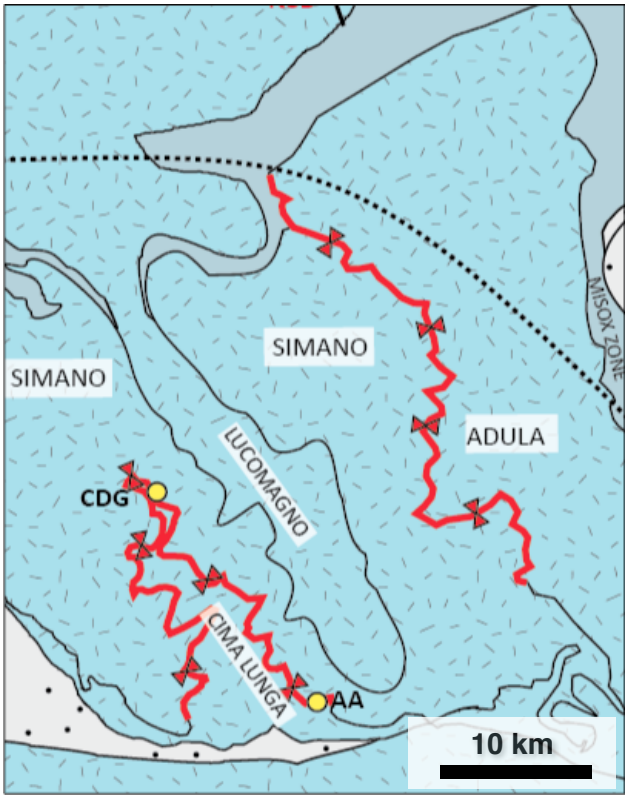

Figure 4.5. The Claro syncline, a D1 structure partially preserved along the Adula-Cima Lunga and Simano contact. This structure is redrawn from Maxelon & Mancktelow (2005), Figure 16.

4.1.3 Reinterpretation of the Simano–Cima Lunga Nappe Contact

Our reinterpretation of the lithological map and cross-section re-opens the discussion of the nappe boundary between the Simano and Adula-Cima Lunga (hereafter Simano–CL) units at Cima di Gagnone. If this entire Lepontine region has been consistently described as deformed by isoclinal D2 folds, then this nappe boundary should be also deformed by D2 folds especially because the Simano–CL nappe boundary was established pre-D2 as defined by the D1 Claro syncline (Maxelon & Mancktelow, 2005). Yet of the most published geological maps do not consider this and trace Simano–CL boundary along the top of the locally-named Verzasca orthogneiss of the Simano nappe (shown Fig. 4.4 as “shear zone”). However, this may simply be a strain boundary, a boundary that separates the little-deformed Verzasca gneiss from the

related mylonites on top (Ramsay and Allison, 1979; Marquer et al., 1996 as cited in Maxelon & Mancktelow, 2005).

In the Alps, it is most common to see north-vergent thrusts or isoclinal recumbent synclines as nappe separators, although they become more ambiguous internal to the orogen. Isoclinal folding can place the same basement rocks (e.g. the Simano and Adula nappe) atop each other, and leaves the nappe boundary as a strongly sheared zone, or a prolongation of the thrust or isoclinal fold hinge (Fig. 4.6; Maxelon & Mancktelow, 2005). The most trustworthy nappe separators are petrographically unambiguous units between nappes. Examples are the Mesozoic sediments that fold into the Penninic nappes but remain petrographically distinct such that they can be used to separate the different units of the Penninic nappe stack (Fig. 2.3). Similarly, within the Upper Penninic nappes, slices of Valaisan metasediments (e.g. Misox zone, Fig. 2.4) define a lithological boundary between the Adula and nappes of the Briançonnais domain.

Following the equivalent criteria for separating the nappes elsewhere in the Penninic nappes, the mafic-ultramafic and marble horizons at Cima di Gagnone may be the real nappe separator (i.e. petrographic unit) marking the boundary between two genetically-similar lithologies: the European basement units of Simano and Adula. As suggested in the previous section, this structure may correspond to the south-closing D1 Claro syncline (Fig. 4.6), whose axial plane traces the current boundary between the Simano and Adula-Cima Lunga nappe (Fig. 4.5). We can interpret these UHP mafic-ultramafic rocks as a separate unit below the Cima Lunga nappe, rather than within in. This is a reasonable interpretation since the UHP rocks are younger (Mesozoic) than the Variscan-aged basement rocks.

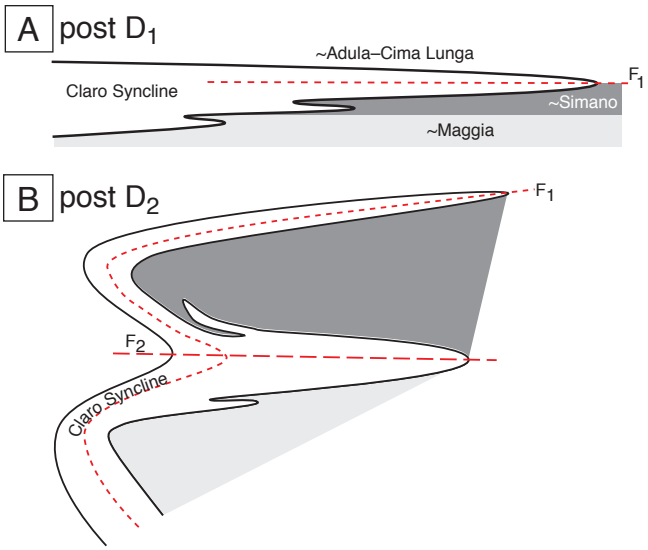

Figure 4.6. Schematic sketch showing the isoclinal Claro syncline. (A) This D1 structure folds the Simano and Adula units atop each other, while the core contains younger (Mesozoic) rocks, which we interpret to be the mafic-ultramafic rocks suite at Cima di Gagnone. (B) The Claro syncline is refolded by the pervasive D2 structures which prolongate and shear the F1 hinges. The D1 structure still separates the Adula unit from the Simano. Figure from Maxelon & Mancktelow (2005).

Alpe Arami

The peridotite and eclogite lens at the Alpe Arami overlies the gneisses of the Simano nappe and is folded in a slight to moderately east-plunging synform (Fig. 3.2; Möckel 1969). The change in foliation and lineation between Cima di Gagnone and Alpe Arami is caused by the general steepening of the structures into the Southern Steep belt. From our observations and interpretation of the more detailed structural observations by Möckel (1969), the main synform of the Alpe Arami is interpreted as a D2 fold with the same structural facing as the D2 folds at the Cima di Gagnone.

4.2 Microstructures

Since the petrography of the field area is very well constrained (e.g. Evans et al., 1981), this study focused on finding shear sense indicators and their associated mineral assemblage.

4.2.1 Microstructural observations

Country rock gneisses

The paragneisses, including pelitic schists, are coarse to medium grained with a mineral assemblage of qtz + pl + bt + ms + grt ± ky ± st. The rocks contain mica-rich domains layered with quartzo-feldspathic domains (Fig. 4.7B). The micas are aligned and define the micro- and macroscopic foliation (S2). Bi-generation garnet porphyroblasts are present; the older generation garnets are subidiomorphic to skeletal and contain numerous inclusions of quartz, feldspars, and micas. The younger generation of garnets tend to be idiomorphic and inclusion-free. The garnet porphyroblast system comprise a Φ-type mantle, capped by the micas, and does not show any systematical shear sense, rather a dominant pure shear deformation (Fig. 4.7A,B).

The orthogneisses, which include the dominant augengneiss, are coarse grained with the mineral assemblage qtz + kfs + pl + bt + ms ± grt. Feldspar porphyroclasts are mantled by myrmekite growth of recrystallized quartz and plagioclase. Some porphyroclasts are rotated, but their sense of rotation were not systematic in the observed samples. Porphyroclast systems show symmetrical Φ-type wings (Fig. 4.7C). Within the shear zone, traditionally mapped as the nappe boundary (Fig 4.4.) there is a striking strain gradient within ~100 m structural thickness marked by a progressive reduction in grain size observed in the orthogneisses in the Simano unit (Samples SM27-30, Fig. 4.8), marked by the disappearance of the kfs augen texture proximal to the Simano–CL contact.

Quartz in all samples show undulose extinction, subgrain rotation, and grain boundary migration recrystallization (Fig. 4.7D). This quartz microstructure is indicative of quartz dynamic

recrystallization above 500 to 550 °C (Stipp et al., 2002). Quartz ribbons are common (Fig. 4.7A, C, D).

Shear bands are observed in the mica-rich samples; they are mostly localized and non-penetrative on the scale of a thin section. The most penetrative shear bands are interpreted as C'-type, are at low angles to the foliation (~20°) and comprise the matrix mineral assemblage (Fig. 4.7F). Other smaller shear bands are localized near porphyroblasts or crystal aggregates; these are unreliable for determining shear sense (Fig. 4.7E).

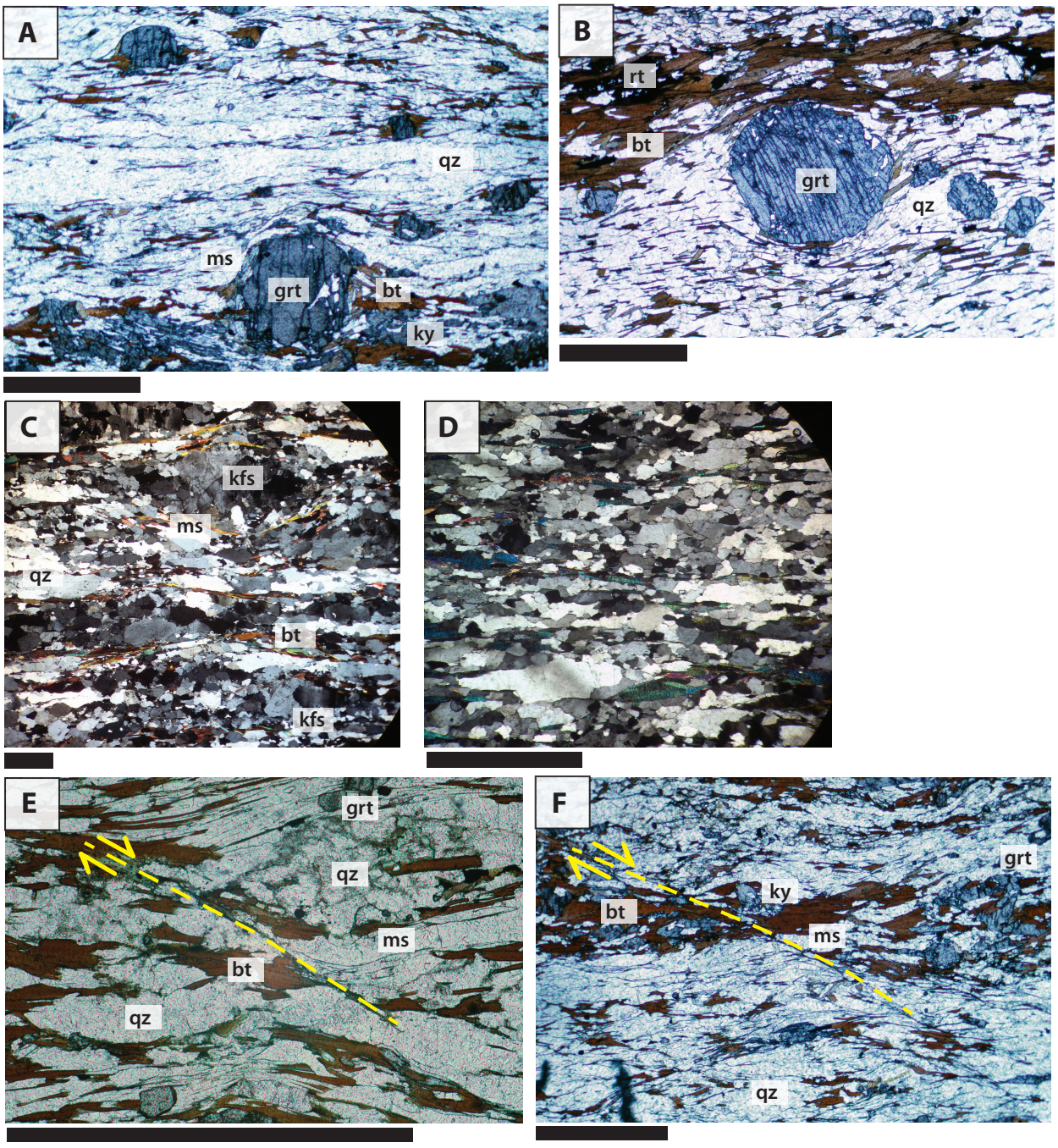

Figure 4.7. (Previous page) Representative photomicrographs of country rock lithologies from Cima di Gagnone; all are taken in PPL except for (C) and (D) taken with in cross polarizers. All the micrographs are oriented such that south is to the right. Scale bar is 2 mm. (A) SM26K: ky-bearing garnet paragneiss and (B) SM14: garnet paragneiss; both photos show a Φ-type mantled porphyroblast of garnet. (C) SM30: Verzasca orthogneiss with Φ-type mantled porphyroclasts of K-feldspar; very coarse grained and elongated kfs porphyroclasts. (D) SM25Q: qz-rich domain of garnet paragneiss showing quartz subgrain formation and grain boundary migration. (E) SM26K, small localized top-to-the-S shear band. (F) SM25: ky-bearing garnet paragneiss with penetrative C'-type, top-to-the-S shear band.

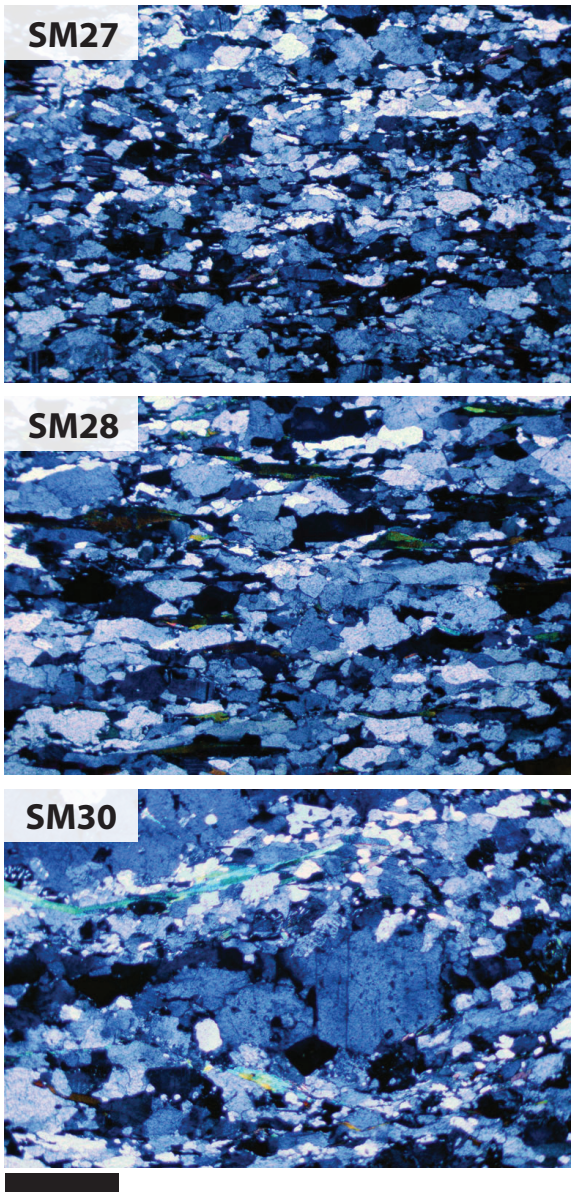

Figure 4.8. Series of photomicrographs showing the progressive grain size reduction in the Simano orthogneiss. All the photomicrographs are taken in XPL and oriented such that south is to the right. Scale bar is 2 mm. The typical orthogneiss shows distinct augen texture (SM30), but we observe a steady decrease in grain size proximal to the Simano-CL contact (SM27). The locations of these sample are shown in Fig. 3.1.

Eclogites and ultramafic-derived rocks

Our eclogite samples show variable degrees of amphibolitization, as confirmed by petrographic observation and EDS data from the SEM-ESBD method. Fresh eclogites appear banded at an outcrop scale (e.g. SM12, Fig. 4.9A); the banding is attributed to compositional variations in eclogite minerals and retrogressive amphibolites and symplectites. A weak foliation can be observed parallel to the banding marked by alignment of pyroxene and hornblende (Fig. 4.9B).

Freshest eclogites have the mineral assemblage grt (prp) + omp ± diop ± rt ± qz, whereas amphibolitized and altered eclogites will contain additional hornblende, clinozoisite, and albite. Fresh eclogites are fine grained, 1-2 mm, where rounded garnets are largest and conspicuous (Fig. 4.10A, B). Omphacite crystals are elongate (Fig. 4.10A and Fig. 4.10B, C) defining the foliation (S1). Two eclogite samples from Alpe Arami show a strong planar fabric defined by elongate garnet and omphacite crystals (Fig. 4.9C, D and Fig. 4.9B, C). Note the presence of an opaque alteration product enveloping garnet and omphacite in altered eclogite samples (Fig. 4.10C, D); this is likely a fine symplectite of albite and amphibole. Composition phase maps from EDS data confirm the major constituent and retrogressive minerals (Fig. 4.11).

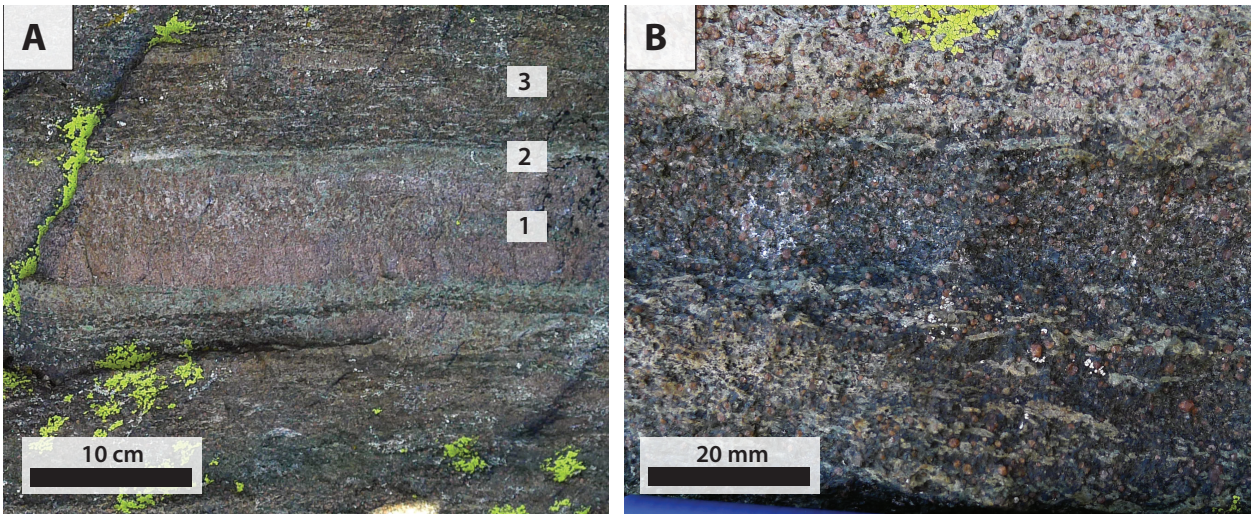

Figure 4.9. Field photo showing layered eclogite, sample SM12, and garnet-amphibolite at the edge of an ultramafic boudin; location of SM12 is shown in Fig. 3.1. Photographs are oriented with south to the right. (A) Banding between eclogite [1] altering to a symplectite after omphacite [2], within garnet-amphibolite [3]. (B) Macro view showing coarse-grained aligned pyroxene and hornblende crystals.

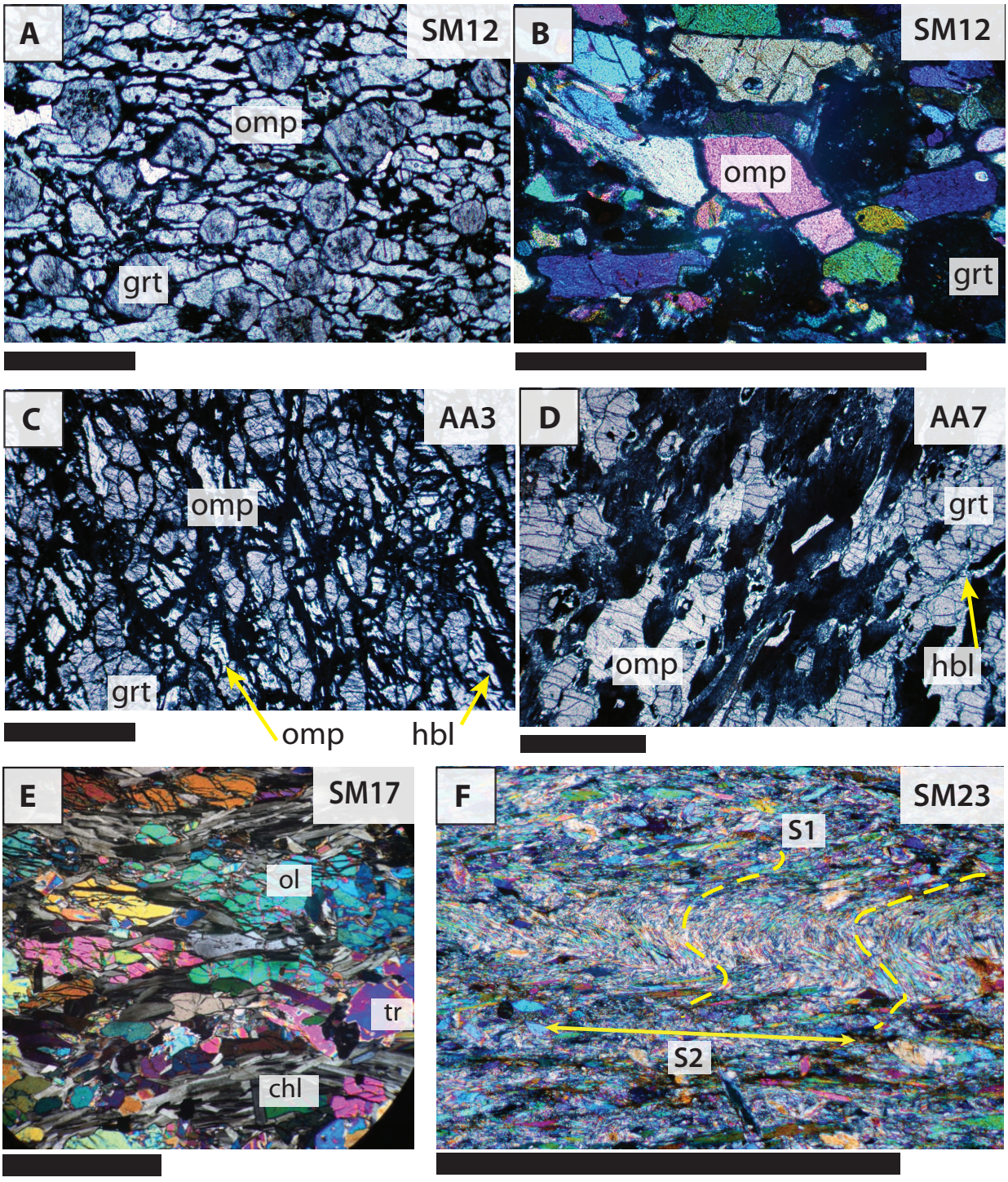

Figure 4.10. Representative photomicrographs of eclogites and ultramafic-derived schists from Cima di Gagnone and Alpe Arami. Scale bar is 2 mm; south is oriented to the right, except in C and D where north is to the right. (A) Eclogite with euhedral pale pink garnet and elongate pale green omphacite crystals in PPL; (B) is the same eclogite shown in XPL. (C), (D) are amphibolitized eclogites showing a distinct opaque alteration product between visible grt + omp + hbl; PPL. (E) Chlorite-tremolite-schist derived from an ultramafic protolith with elongate olivine crystals and chlorite defining a foliation; XPL. (F) Talc schist showing crenulation cleavage and evidence for earlier deformation (S1); XPL.

Other non-eclogite samples include schists that are associated with the hydrous alteration of ultramafic bodies nearby; they have a general mineral assemblage of ol + di + tlc + chl + srp ± tr. Samples were collected at the contact between an ultramafic boudin and its paragneiss host. Foliation in these ultramafic-derived schists are defined by olivine, chlorite, and/or talc (Fig. 4.9E, F). A very fine-grained talc schist sample shows crenulation cleavage and evidence for S1, preserved locally between the pervasive S2 fabric (Fig. 4.9F).

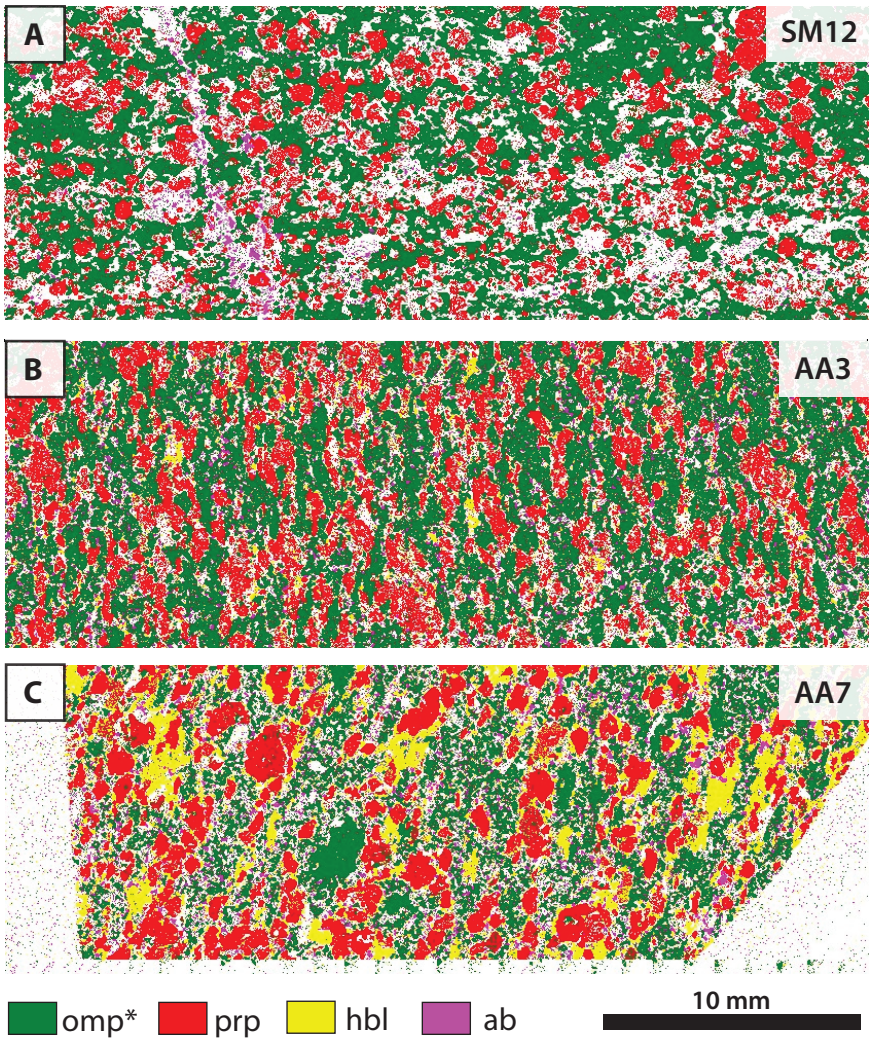

Figure 4.11. Composition phase maps constructed with EDS data. The three samples correspond to those showing suitable omphacite LPO fabric (described in Ch. 5.1). Pyrope and omphacite are the dominant mineral phases, along with hornblende in (B) 8 % and (C) 15 %. Albite is present in all three samples at <6 %. * *The EDS system indexed omphacite under diopside due to an error in the reference database of the ESBD software for omphacite.*

4.2.2 Discussion

Microstructures of orthogneisses and paragneisses indicate dominant pure shear (or sub-simple shear) deformation during the D2, which is consistent with the regional-scale structures (e.g. isoclinal recumbent folds, crenulation cleavage). Eclogite and related ultramafic samples do not show any microstructures that can be associated with deformation geometry. We can suspect that the strong fabric observed in the Alpe Arami samples (Fig. 4.11B, C) may be related to pure shear deformation; this was tested with ESBD and will be discussed in the following chapter.

4.3 Summary of (Micro)structural Observations

The Adula and Simano nappes are in direct contact only in the absence of Mesozoic cover sediments in the southern Adula-Cima Lunga region, including at Cima di Gagnone (Fig. 2.4). As such, we expected to find evidence for thrusting or shearing that would represent the emplacement of the Adula-Cima Lunga nappe atop the Simano nappe, a boundary that was documented as a mylonitic zone (Fig. 4.4; Partzsch 1998, as cited in Rütti 2005). The conspicuous mylonite zone at the conventional Simano–Cima Lunga nappe boundary consist of mylonitic to protomylonitic Verzasca gneiss. However, no asymmetric structures were found neither at outcrop nor at the microscopic scale (e.g. Fig. 4.8). The grain boundary migration recrystallization in quartz combined with myrmekite growth at K-feldspar boundaries indicate deformation temperatures above 600 °C (Passchier and Trouw 2005, and references therein). The Adula and Simano nappes were interpreted to have welded together prior to D2, since isoclinal D2 folds overprint the nappe contact (Rütti 2005; Nagel et al., 2002a; Nagel et al., 2002b). So any shear sense found in the Adula or Simano ortho- and paragneisses would have been attributed to the D2 stage which accommodated decompression from the HP stage. However, in our samples, these rocks show a significant component of pure shear deformation

(i.e. non-rotational strain). Our observations also cannot support or refute tectonic accretion channel model.

The lack of microstructural evidence for simple shear deformation can be attributed to the overprinting of D1 fabric by the pervasive D2 structures during the HT Lepontine metamorphic event. Whereas previous studies on the Simano–Adula nappe contact were conducted further east in the main Adula nappe (e.g. Rütti 2005), the Cima di Gagnone locality appears to have either experienced more intensive D2 deformation, or did not experience the same nappe emplacement history.

Chapter 5: Textures

5.1 ESBD Results

Pole figures for all ESBD analyses are presented in Appendix A. Although textural analyses were performed on 14 samples, only three samples showed a clear omphacite LPO pattern. These are presented and described below (Fig 5.1).

SM12

Sample SM12 from Cima di Gagnone shows distinct LPO pattern characterized by a concentration of (010)-poles perpendicular to XY (i.e. foliation) and a diffuse girdle of [001]-axes oriented parallel to XY. The [100]-axes and (110)-poles show a very weak and broad girdle parallel and perpendicular to X (i.e. lineation), respectively. Based on the strong signals of the (010) and [001] LPO, sample SM12 resembles a transitional SL-type deformation fabric (Helmstaedt et al., 1972), with slight affinity for the S-type flattening fabric (Fig. 3.6).

AA3

Sample AA3 from Alpe Arami shows concentrated (010)-poles perpendicular to XY and maxima of [001]-axes connected by a weak girdle parallel to X. The (110)-poles show a weak and broad girdle perpendicular to X, and the [001]-axes show a diffuse concentration parallel to X, lying within the XY plane. The (010)-poles show affinity for the S-type point maxima but the [001]-axes resemble an intermediate girdle to point maxima pattern in between the S- and L-type. Overall, this sample also resembles a transitional LS-type deformation fabric.

AA7

Sample AA7 from Alpe Arami shows a weaker LPO pattern compared to the previous samples. It is characterized by concentrated [001]-axes parallel to X and a diffuse girdle of (010)-poles

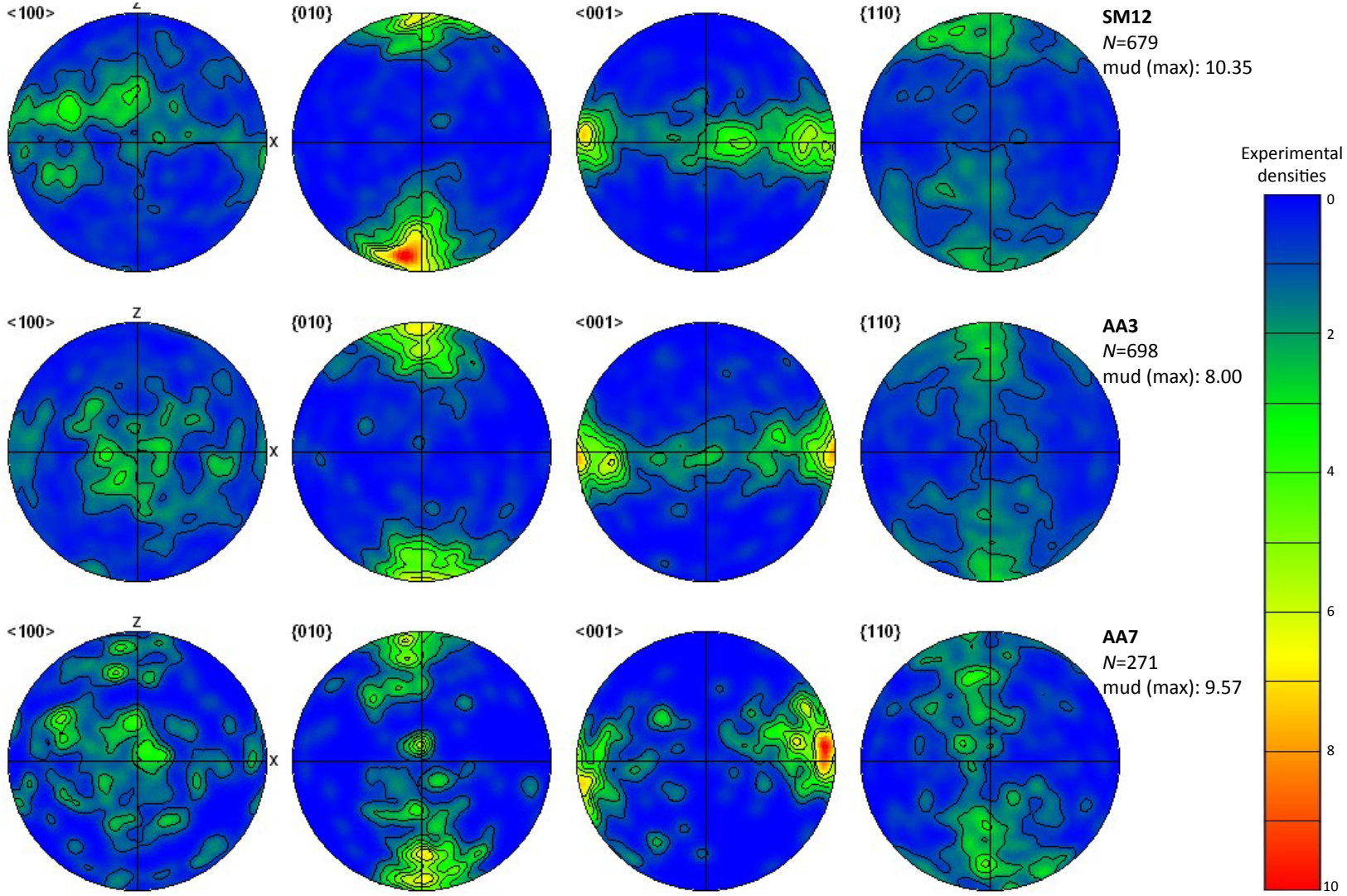

Figure 5.1. Pole figures showing omphacite LPO measured using the ESBD technique. Four pole figures for each sample show orientations of the <100> and <001> axes, and the {010} and {110} planes. Equal area projection, lower hemisphere. Concentrations are relative experimental densities (mud): minimum=0.00, maximum=10.35. Contours at 1, 2, 3, ...6 mud. N: number of data points where each data point represents one indexed diopside grain (>200 um).

sub-perpendicular to X. The (110)-poles show a weak and broad girdle perpendicular to X, and [100]-axes show an indistinct fabric pattern. This sample also resembles the transitional LS-type, but shows affinity for the L-type constrictional fabric because the (010)-poles form a relatively stronger girdle than the [001]-axes.

The LPO patterns with the strongest densities are within the pole figures for [001] and (010); this corresponds to activity on the [001]{110} slip system, which is dominant during deformation under moderate to high temperatures (Ch. 3.4.1).

Poor quality LPO patterns

As an example, Figure 5.2 shows two samples with poor quality LPO patterns. In both examples, the [001]-axes show a tendency for a girdle parallel to the foliation while the [100]-axes and (010)-poles have a maximum perpendicular to lineation. These patterns, however, are very diffuse with low experimental densities; although they demonstrate a very weak LPO fabric, such samples will not be used for further interpretation in this study.

Poor LPO patterns may be due to an improper cut from the hand sample; SM04A, a coarse-grained sample, was perhaps not cut perpendicular to the foliation or parallel to lineation. To improve the quality of LPO patterns, both samples should be re-cut to ensure the proper kinematic plane and then re-scanned at a higher spatial resolution.

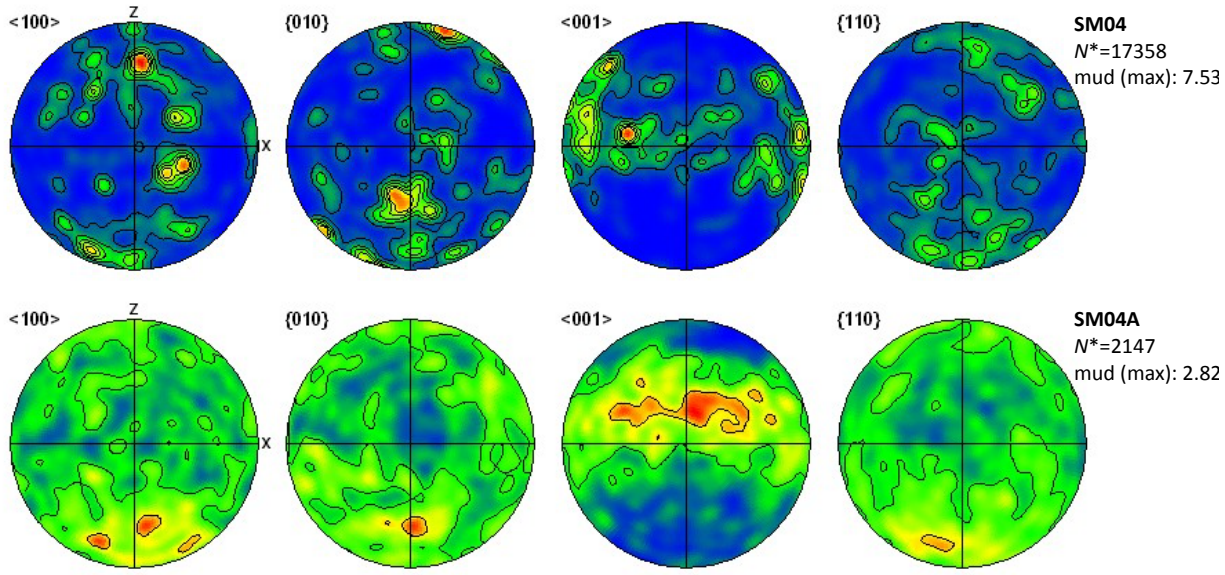

Figure 5.2. Pole figures showing examples of poor LPO patterns of omphacite. These LPO patterns are ambiguous and implies the absence of LPO in omphacite at this scale of observation. Pole figure parameters are the same as in Fig. 5.1. *N**: number of *scanned* points (i.e. size bias was not considered).

5.2 Discussion

Our textural data from three localities across the Adula-Cima Lunga nappe do not show end-member omphacite LPO fabric. All three samples (SM12, AA3, AA7) have intermediate LS-type fabrics, which is interpreted as a transitional fabric between the flattening and constriction (Helmstaedt et al., 1972; Kurz et al., 2004). Activity on the high temperature [001]{110} slip system was expected as these are (U)HP rocks.

The type of omphacite LPO fabric has tectonic implications; the textural evolution of omphacite is strongly related to deformation geometry during high pressure to exhumation conditions (Bascou et al., 2002; Godard & van Roermund, 1995). L-type fabric of constrictional strain geometry is associated with peak and post-peak pressure conditions and early stages of exhumation in the subduction channel, whereas S-type fabric of flattening strain geometry is associated with compression during subduction or exhumation by crustal thinning and extension (Kurz et al., 2004).

5.3 Textural Contrast between the Adula and Cima Lunga Units

Studies by Pleuger et al. (2003) and Kurz et al. (2004) show consistent L-type fabric for eclogite rocks from the main Adula nappe. The L-type fabric the main Adula indicate constrictional deformation during HP eclogite facies conditions to the earliest stages of exhumation; some samples also show asymmetry indicating non-coaxial deformation during this stage (Kurz et al., 2004). Textural data from eclogite rocks at Alpe Arami (Cima Lunga unit) show variable results: Kurz et al. (2004) found S>L-type flattening fabric, while Bascou et al. (2001) found L-type or L>S-type constrictional fabric. The samples from all previous studies, however, are not referenced to geographic coordinates and the regional shear sense is not known.

Textural measurements in this study enhance the contrast in omphacite texture between the two sections of the Adula-Cima Lunga nappe. The top of the Adula nappe is characterized by L-type fabric, while the Cima Lunga unit at the base of the Adula is characterized by the L-S and S>L-type fabric (Fig. 5.1). The spatial variation in omphacite texture from the main Adula nappe to the Cima Lunga unit suggests that these two sections may have experienced a different deformation history.

5.4 Tectonic Implications

Comparison of geochronological data between the main Adula nappe and the Cima Lunga unit show age discrepancies for the (U)HP mafic-ultramafic rocks and their country rocks (Ch. 2.4). This supports the notion that they have experienced different geodynamic histories.

The main Adula nappe has experienced a late Paleozoic Variscan HP metamorphic event that was detected in both country rock gneisses *and* eclogites (Herwartz et al., 2011; Liati et al., 2009), which indicates that they must have became a coherent unit post-Variscan deformation and prior to Alpine subduction. The same statement cannot be made for the Cima Lunga unit, because although the orthogneisses yield Variscan ages, no pre-Alpine ages in the

paragneisses, marbles, and mafic-ultramafic rocks have been found. This is because the protoliths to these metasedimentary and meta-mafic-ultramafic rocks are Mesozoic in age, and therefore these rocks stratigraphically and paleogeographically represent the Valais ocean basin sediments and mantle rocks. Ages for Alpine HP metamorphism, ca. 35-38 Ma, are found in eclogites of both the main Adula nappe and Cima Lunga unit to approximate HP and UHP conditions, respectively. The 33-34 Ma age found throughout the Adula-Cima Lunga nappe represents the HT Lepontine metamorphism where country rock gneisses and their mafic-ultramafic rocks behaved as one coherent unit during exhumation from mid-crustal levels.

Although the Alpine HP event was detected in the main Adula nappe, it likely was not subducted to the same depths as the Cima Lunga unit as suggested by thermobarometric constraints. The 38 Ma age from Herwartz et al. (2011) at Trescolmen corresponds to a peak pressure of 22 kbar (Ch. 2.3.3; Dale & Holland, 2003); the ~38 Ma age (Brouwer et al., 2005) from eclogites near Gorduno (near Alpe Arami) corresponds to 23 kbar (Tóth et al., 2000), whereas similar 37-38 Ma ages from Cima di Gagnone and Alpe Arami were interpreted to correspond to UHP conditions of 30-35 kbar (Becker, 1993).

Along with the omphacite texture data from this study and previous studies, we see that the geochronological data for (U)HP conditions also point to a difference between the main Adula nappe and the Cima Lunga unit in terms of its tectonic environment during the peak pressure stage. We can suggest the following:

- Prior interpretations of the Adula nappe behaving as a coherent unit are relevant for only the Alpine event, and applies to the main Adula nappe exclusive of the Cima Lunga unit.

    a. The mafic and ultramafic rocks of the Cima Lunga unit (whose protoliths are Mesozoic in age) were subducted to UHP depths at ~37-38 Ma, as supported by petrographic, thermobarometric, and geochronological data. Their country rock gneisses show no evidence for (U)HP metamorphism; thus, the eclogites and ultramafics must have been incorporated into their host rocks in the subduction channel during subduction and/or

exhumation as a lithospheric mélange, presumably at or prior to 33 Ma (Gebauer, 1996). Alternatively, if we view these mafic-ultramafic rocks as a nappe separating unit, then they were emplaced between basement gneisses at or prior to 33 Ma. This is in agreement with the petrography of the Cima Lunga mafic-ultramafic rocks that suggest a shallow Valaisan ocean floor paleogeographic setting, prior to Alpine subduction.

b. It is unlikely that the main Adula nappe was subducted to UHP depths during the Alpine event because the overall unit is volumetrically dominated by buoyant crustal rocks (gneisses of the European continent), which are difficult to subduct to the same UHP depths as the dense Cima Lunga eclogitic and ultramafic rocks. Within the main Adula nappe, eclogites show peak Alpine pressures between 13-24 kbar (see references in Section 2.2.4). In Alpe Arami, eclogites yield peak pressures of 23±3 kbar. Higher pressures (i.e. UHP, >25 kbar) are found within ultramafic rocks (garnet lhzerzolites and peridotites) at Mont Duria and within the Cima Lunga localities.

- The observed S>L- to L-S-type omphacite LPO fabric from this study and previous studies can be attributed to a flattening strain geometry, which is concordant with our microstructural observations for pure shear. According to Kurz et al. (2004) and Nagel (2000), these observations may suggest that an important component of exhumation of the Cima Lunga HP rocks was achieved by pure shear, through vertical thinning and horizontal lengthening. This would be accompanied by strong sub-horizontal planar fabric and sub-horizontal isoclinal folds with hinges parallel to the prominent NNW-SSE stretching lineation. This is concordant with our preliminary field observations.

In summary, these conclusions strengthen the idea that the Cima Lunga unit (i.e. the core of the Claro syncline) can be considered as a separate lithotectonic unit from the main Adula nappe.

Chapter 6: Conclusions and Recommendations

6.1 Conclusions

In an area that has been studied extensively for its (U)HP rocks and complex deformation history, our structural and textural observations strengthen the contrast between the main Adula nappe and the Cima Lunga unit in terms of their geodynamic history. Although our original intent was to analyze the exhumation kinematics of (U)HP eclogite rocks and their host rocks, our microstructural observations lacked evidence for simple shear, but instead revealed a significant component of pure shear deformation. Textural data from omphacite LPO in eclogite samples show a transitional LS-type to S>L-type fabric indicative of an deformation geometry intermediate between constriction and flattening, with tendency for flattening at Cima di Gagnone. We can suggest that the UHP eclogite and ultramafic rocks from Cima di Gagnone and Alpe Arami underwent pure shear deformation with affinity for flattening strain geometry. With our observations and interpretations, we can suggest that exhumation was facilitated by the extreme nappe-internal thinning tectonic model (Nagel, 2008), where exhumation is achieved by strong vertical thinning with strain conditions close to that of pure shear flattening.

Field observations and structural mapping contribute to defining the nappe boundary between the Cima Lunga unit and the underlying Simano nappe of the lower Penninic nappes. With knowledge of the complex deformation history in the Penninic nappes, especially within the Lepontine dome, we re-interpreted the nappe boundary between the Simano and Cima Lunga. Since HP metamorphism has never been detected in the Variscan-aged host gneisses of Cima Lunga and Simano units, we are guided to interpret the mafic-ultramafic rock suite as a nappe separating unit situated at the base of the Cima Lunga continental basement unit, i.e. the core of a south-closing syncline with Mesozoic lithologies separating Variscan basement nappes. This interpretation is concordant with deformation geometries of multiple folding events (D1-D4), and by virtue that the protoliths of the mafic-ultramafic rock suite are Mesozoic-aged rocks derived from the Valais ocean basin.

With further investigation, we find subtle but contrasting geochronological and thermobarometric data for the mafic-ultramafic bodies and country rock gneisses between the Cima Lunga unit and the main Adula nappe. The main Adula nappe has experienced two subduction cycles: Variscan and Alpine. The UHP mafic-ultramafic rocks were emplaced into continental rocks (i.e. Adula) during Variscan orogeny. The Alpine subduction event only reached HP conditions where the Adula was subducted and exhumed as a coherent unit. The main Adula nappe did not reach the UHP conditions that were reported in the Cima Lunga mafic-ultramafic rocks. Interestingly enough, the Cima Lunga unit only records the Alpine subduction cycle in its UHP rocks, while lower-pressure country rocks only show Variscan protolith ages and Lepontine high-temperature-low pressure metamorphism. The mafic-ultramafic units of Cima Lunga experienced subduction into UHP depths and were emplaced between continental host rocks at mid-crustal levels during its exhumation. With our omphacite LPO data, we can suggest that the Cima Lunga UHP rocks were exhumed with significant pure shear deformation, through crustal thinning and extension.

This study presents insight into a contrasting geodynamic history between the main Adula nappe and the Cima Lunga unit. With field, microstructural, and textural data from this study and a thorough review of published data, we suggest that the Cima Lunga unit may be a separate lithotectonic unit from the main Adula nappe, whereby only the former was subducted to UHP conditions during Alpine orogeny.

6.2 Recommendations for Further Study

1. *Geochronology and thermobarometry.* These methods allow for further examination of the mafic-ultramafic and country rock association in the Cima Lunga; results can be used for comparison to the well-established studies in the main Adula nappe. Systematic sampling of the eclogite and garnet peridotite for SHRIMP zircon dating and Lu-Hf dating of garnet should be undertaken to establish the temporal relationship between the UHP eclogite rocks (crustal-

derived) and the ultramafic rocks (mantle-derived) during the Alpine subduction and exhumation. Currently in the Cima Lunga unit, all available geochronological data are obtained from ultramafic garnet peridotites; it would be worthwhile to investigate whether the MORB-derived eclogites were subducted to the same UHP depths as ultramafic mantle-derived rocks (e.g. garnet peridotites and lherzolites). Will the mafic eclogites yield the same P-T-t conditions as the ultramafic rocks?

2. *Omphacite textures.* ESBD should be performed at a higher resolution to refine the omphacite LPO results for all eclogite samples. The SEM-ESBD system was capable of high-resolution mapping at 1 μm; a higher resolution would yield higher density of scan points, such that the omphacite grains can be better defined. More data points can lessen the effect of size bias (when several large grains dominate the data set), and thus, improve the statistics of the textural data.

3. *Olivine textures*. The ESBD technique can also be used to examine olivine texture in deformed and undeformed ultramafic rocks to see if they are compatible with eclogite textures.

References

Bascou, J., Barruol, G., Vauchez, A., Mainprice, D., & Egydio-Silva, M. (2001). EBSD-measured lattice-preferred orientations and seismic properties of eclogites. *Tectonophysics*, *342*(1), 61–80.

Bascou, J., Tommasi, A., & Mainprice, D. (2002). Plastic deformation and development of clinopyroxene lattice preferred orientations in eclogites. *Journal of Structural Geology*, *24*(8), 1357–1368.

Becker, H. (1993). Garnet peridotite and eclogite Sm-Nd mineral ages from the Lepontine dome (Swiss Alps): New evidence for Eocene high-pressure metamorphism in the central Alps. *Geology*, *21*(7), 599–602.

Bousquet, R., Oberhansli, R., Goffe, B., Wiederkehr, M., Koller, F., Schmid, S. M., et al. (2008). Metamorphism of metasediments at the scale of an orogen: a key to the Tertiary geodynamic evolution of the Alps. *Geological Society, London, Special Publications*, *298*(1), 393–411. doi:10.1144/SP298.18

Brouwer, F. M., Burri, T., Engi, M., & Berger, A. (2005). Eclogite relics in the Central Alps: PT-evolution, Lu–Hf ages and implications for formation of tectonic mélange zones. *Schweizerische Mineralogische Und Petrographische Mitteilungen*, *85*, 147–174.

Carswell, D. A., & Zhang, R. Y. (2000). Petrographic characteristics and metamorphic evolution of ultrahigh-pressure eclogites in plate-collision belts. *Ultra-High Pressure Metamorphism and Geodynamics in Collision-Type Orogenic Belts*, *4*, 39–56.

Chopin, C. (1984). Coesite and pure pyrope in high-grade blueschists of the Western Alps: a first record and some consequences. *Contributions to Mineralogy and Petrology*, *86*(2), 107–118.

Chopin, Christian, Caroline Henry, and Andre Michard. "Geology and petrology of the coesite-bearing terrain, Dora Maira massif, Western Alps." *European Journal of Mineralogy* 3, no. 2 (1991): 263-291.

Chopin, C. (2003). Ultrahigh-pressure metamorphism: tracing continental crust into the mantle. *Earth and Planetary Science Letters*, 212(1), 1–14. doi:10.1016/S0012-821X(03)00261-9

Dale, J., & Holland, T. J. B. (2003). Geothermobarometry, P-T paths and metamorphic field gradients of high-pressure rocks from the Adula Nappe, Central Alps. *Journal of Metamorphic Geology*, *21*(8), 813–829. doi:10.1046/j.1525-1314.2003.00483.x

Engi, M., Berger, A., & Roselle, G. T. (2001). Role of the tectonic accretion channel in collisional orogeny. *Geology*, *29*(12), 1143–1146.

Evans, B. W., Trommsdorff, V., & Goles, G. G. (1981). Geochemistry of high-grade eclogites and metarodingites from the Central Alps. *Contributions to Mineralogy and Petrology*, *76*(3), 301–311.

Evans, B. W., Trommsdorff, V., & Richter, W. (1979). Petrology of an eclogite-metarodingite suite at Cima di Gagnone, Ticino, Switzerland. *American Mineralogist*, *64*(1-2), 15–31.

Ernst, W. G., B. R. Hacker, and J. G. Liou. "Petrotectonics of ultrahigh-pressure crustal and upper-mantle rocks—implications for Phanerozoic collisional orogens." Geological Society of America Special Papers 433 (2007): 27-49.

Frisch, W. (1981). Plate motions in the Alpine region and their correlation to the opening of the Atlantic ocean. *Geologische Rundschau*, *70*(2), 402–411.

Froitzheim, N., Schmid, S. M., & Frey, M. (1996). Mesozoic paleogeography and the timing of eclogite-facies metamorphism in the Alps: a working hypothesis. *Eclogae Geologicae Helvetiae*, *89*(1), 81–&.

Gebauer, D. (1996). A PTt path for an (ultra?-) high-pressure ultramafic/mafic rock-association and its felsic country-rocks based on SHRIMP-dating of magmatic and metamorphic zircon domains. Example: Alpe Arami (Central Swiss Alps). *Geophysical Monograph Series*, *95*, 307–329.

Godard, G., & van Roermund, H. L. (1995). Deformation-induced clinopyroxene fabrics from eclogites. *Journal of Structural Geology*, *17*(10), 1425–1443.

Grond, R., Wahl, F., & Pfiffner, M. (1995). Polyphase Alpine deformation and metamorphism in the northern Cima Lunga unit, Central Alps (Switzerland). *Schweizerische Mineralogische Und Petrographische Mitteilungen*, *75*, 371–386. doi:10.5169/seals-57162

Grujic, D, & Mancktelow, N. S. (1996). Structure of the norther Maggia and Lebendun Nappes, Lepontine Alps, Switzerland. *Eclogae Geologicae Helvetiae, 89*(1), 461-504.

Helmstaedt, H., Anderson, O. L., & Gavasci, A. T. (1972). Petrofabric studies of eclogite, spinel-websterite, and spinel-lherzolite Xenoliths from kimberlite-bearing breccia pipes in southeastern Utah and northeastern Arizona. *Journal of Geophysical Research*, *77*(23), 4350–4365.

Herwartz, D., Nagel, T. J., Münker, C., Scherer, E. E., & Froitzheim, N. (2011). Tracing two orogenic cycles in one eclogite sample by Lu-Hf garnet chronometry. *Nature Geoscience*, *4*(3), 178–183. doi:10.1038/ngeo1060

Janák, M., Froitzheim, N., Lupták, B., Vrabec, M., & Ravna, E. J. K. (2004). First evidence for ultrahigh-pressure metamorphism of eclogites in Pohorje, Slovenia: Tracing deep continental subduction in the Eastern Alps. *Tectonics*, *23*(5), n/a–n/a. doi:10.1029/2004TC001641

Kretz, R. (1983). Symbols for rock-forming minerals. *American Mineralogist, 68,* 277-279.

Kurz, W., Jansen, E., Hundenborn, R., Pleuger, J., Schäfer, W., & Unzog, W. (2004). Microstructures and crystallographic preferred orientations of omphacite in Alpine eclogites: implications for the exhumation of (ultra-) high-pressure units. *Journal of Geodynamics*, *37*(1), 1–55. doi:10.1016/j.jog.2003.10.001

Liati, A., Gebauer, D., & Fanning, C. M. (2009). Geochronological evolution of HP metamorphic rocks of the Adula nappe, Central Alps, in pre-Alpine and Alpine subduction cycles. *Journal of the Geological Society*, *166*(4), 797–810. doi:10.1144/0016-76492008-033

Mauler Steinmann, A. (2000). Texture and Microstructures in Eclogites. EBSD applied to Samples from Nature and Experiment. PhD Dissertation, ETH, no. 12690 1–7.

Maxelon, M., & Mancktelow, N. S. (2005). Three-dimensional geometry and tectonostratigraphy of the Pennine zone, Central Alps, Switzerland and Northern Italy. *Earth-Science Reviews*, *71*(3-4), 171–227. doi:10.1016/j.earscirev.2005.01.003

Merle, O., Cobbold, P. R., & Schmid, S. (1989). Tertiary kinematics in the Lepontine dome. *Geological Society, London, Special Publications*, *45*(1), 113–134. doi:10.1144/GSL.SP.1989.045.01.06

Moeckel, J. R. (1969). Structural petrology of the garnet-peridotite of Alpe Arami (Ticino, Switzerland). *Leidse Geologische Mededelingen*, 42, 61–130.

Nagel, T. J. (2008). Tertiary subduction, collision and exhumation recorded in the Adula nappe, central Alps. *Geological Society, London, Special Publications*, *298*(1), 365–392. doi: 10.1144/SP298.17

Nagel, T. J., de Capitani, C., & Frey, M. (2002a). Isograds and P-T evolution in the eastern Lepontine Alps (Graubuden, Switzerland). *Journal of Metamorphic Geology*, 20, 309–324.

Nagel, T. J., de Capitani, C., & Frey, M. (2002b). Structural and metamorphic evolution during rapid exhumation in the Lepontine dome (southern Simano and Adula nappes, Central

Alps, Switzerland). *Eclogae Geologicae Helvetiae*, *95*, 301–321. doi:10.5169/seals-168962

Neufeld, K., Ring, U., Heidelbach, F., Dietrich, S., & Neuser, R. D. (2008). Omphacite textures in eclogites of the Tauern Window: Implications for the exhumation of the Eclogite Zone, Eastern Alps. *Journal of Structural Geology*, 30(8), 976–992. doi:10.1016/j.jsg.2008.03.010

Nicolas, A., & Poirier, J. P. (1976). *Crystalline plasticity and solid state flow in metamorphic rocks*. New York: Wiley.

Nimis, P., & Trommsdorff, V. (2001). Revised thermobarometry of Alpe Arami and other garnet peridotites from the Central Alps. *Journal of Petrology*, *42*(1), 103–115.

Paquin, J., & Altherr, R. (2001). New constraints on the P–T evolution of the Alpe Arami garnet peridotite body (Central Alps, Switzerland). *Journal of Petrology*, *42*(6), 1119–1140.

Passchier, C. W., & Trouw, A. J. (2005). *Micro-tectonics*. Springer-Verlag: Berlin Heidelberg, Germany.

Pfiffner, M., & Trommsdorff, V. (1998). The high-pressure ultramafic-mafic-carbonate suite of Cima Lunga-Adula, Central Alps: Excursions to Cima di Gagnone and Alpe Arami. *Schweizerische Mineralogische Und Petrographische Mitteilungen*, *78*(2), 337–354. doi:10.5169/seals-59292

Ramsay, J. G. & Huber, M. I. (1987). *The techniques of modern structural geology. Volume 2: Folds and fractures*. Academic Press: London, United Kingdom.

Rice, J. M. (1983). Metamorphism of rodingites: Part I, phase relations in a portion of the system CaO-MgO-Al2O3-SiO2-CO2-H2O. *American Journal of Science,* col 283-A, 121-150.

Rosenbaum, G., Lister, G. S., & Duboz, C. (2002). Relative motions of Africa, Iberia and Europe during Alpine orogeny. *Tectonophysics*, *359*(1), 117–129.

Rütti, R., Maxelon, M., & Mancktelow, N. S. (2005). Structure and kinematics of the northern Simano Nappe, Central Alps, Switzerland. *Eclogae Geologicae Helvetiae*, 98(1), 63–81. doi:10.1007/s00015-005-1148-7

Schmid, S. M., Fugenschuh, B., Kissling, E., & Schuster, R. (2004). Tectonic map and overall architecture of the Alpine orogen. *Eclogae Geologicae Helvetiae*, *97*(1), 93–117. doi: 10.1007/s00015-004-1113-x

Schmid, S. M., Pfiffner, O. A., Froitzheim, N., Schönborn, G., & Kissling, E. (1996). Geophysical-geological transect and tectonic evolution of the Swiss-Italian Alps. *Tectonics*, *15*(5), 1036–1064.

Smith, D. C. (1984). Coesite in clinopyroxene in the Caledonides and its implications for geodynamics. *Nature Publishing Group*, *310*, 641–644.

Stipp, M., Stunitz, H., & Heilbronner, R. (2002). The eastern Tonale fault zone: a “natural laboratory” for crystal plastic deformation of quartz over a temperature range from 250 to 700 °C. Journal of Structural Geology.

Tóth, T. M., Grandjean, V., & Engi, M. (2000). Polyphase evolution and reaction sequence of compositional domains in metabasalt: a model based on local chemical equilibrium and metamorphic differentiation. *Geological Journal*.

Trommsdorff, V., Hermann, J., Müntener, O., Pfiffner, M., & Risold, A.-C. (2000). Geodynamic cycles of subcontinental lithosphere in the Central Alps and the Arami enigma. *Journal of Geodynamics*, *30*(1), 77–92.

Twiss, R. J. & Moore, E. M. (2006). *Structural Geology*. W. H. Freeman: USA.

Ulrich, S., & Mainprice, D. (2005). Does cation ordering in omphacite influence development of lattice-preferred orientation? *Journal of Structural Geology*, *27*(3), 419–431. doi:10.1016/j.jsg.2004.11.003

Zhang, J., Greenii, H., & Bozhilov, K. (2006). Rheology of omphacite at high temperature and pressure and significance of its lattice preferred orientations. *Earth and Planetary Science Letters*, *246*(3-4), 432–443. doi:10.1016/j.epsl.2006.04.006

Appendix 1

Cima di Gagnone pole figures for diopside/omphacite. A grain size filter of greater than 200 um diameter (circle equivalent) was applied to all samples. Sample name and all other processing parameters are listed in the right-hand side panel and are equivalent for each sample, with the exception of the gradient scale that is relative to each sample's experimental density (mud value).

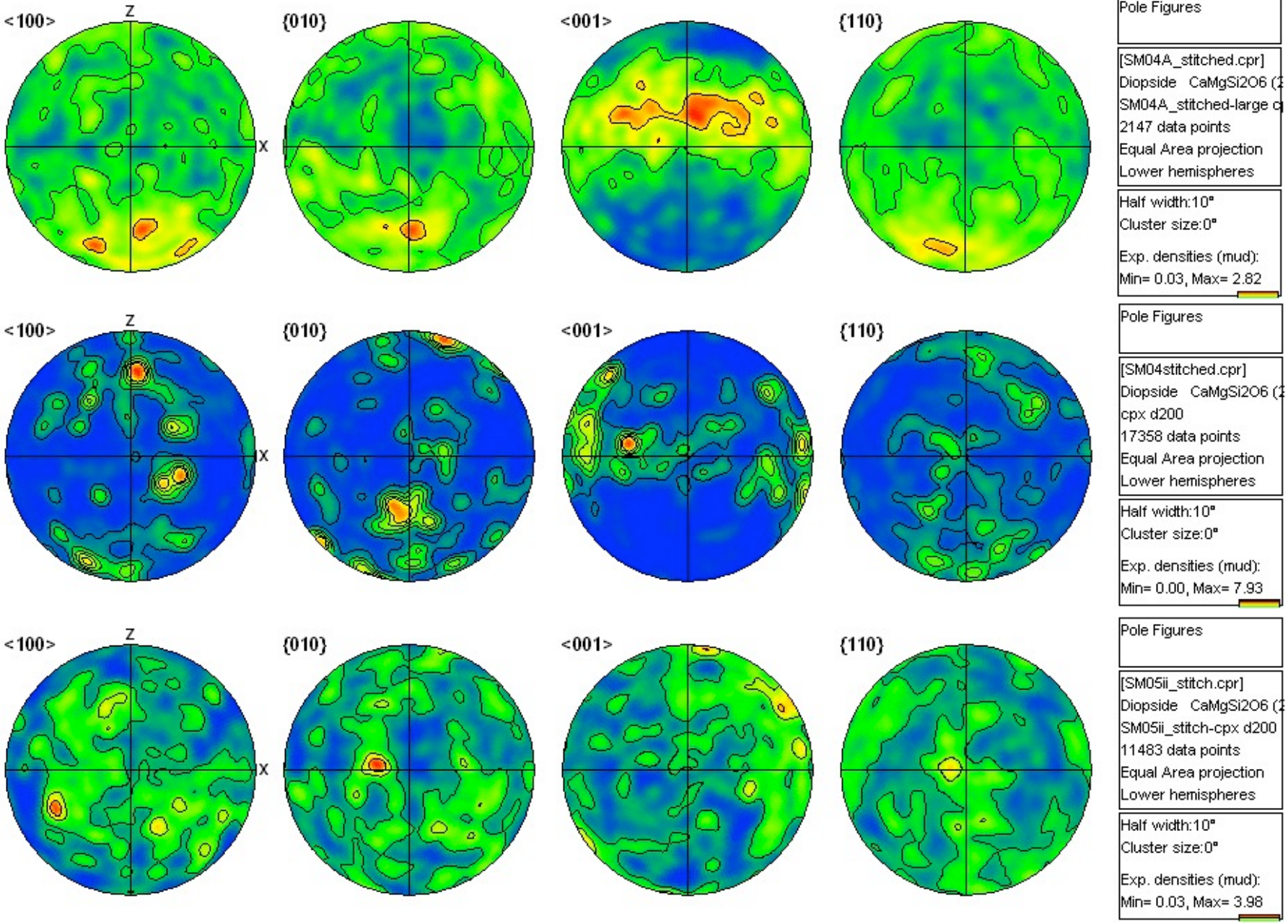

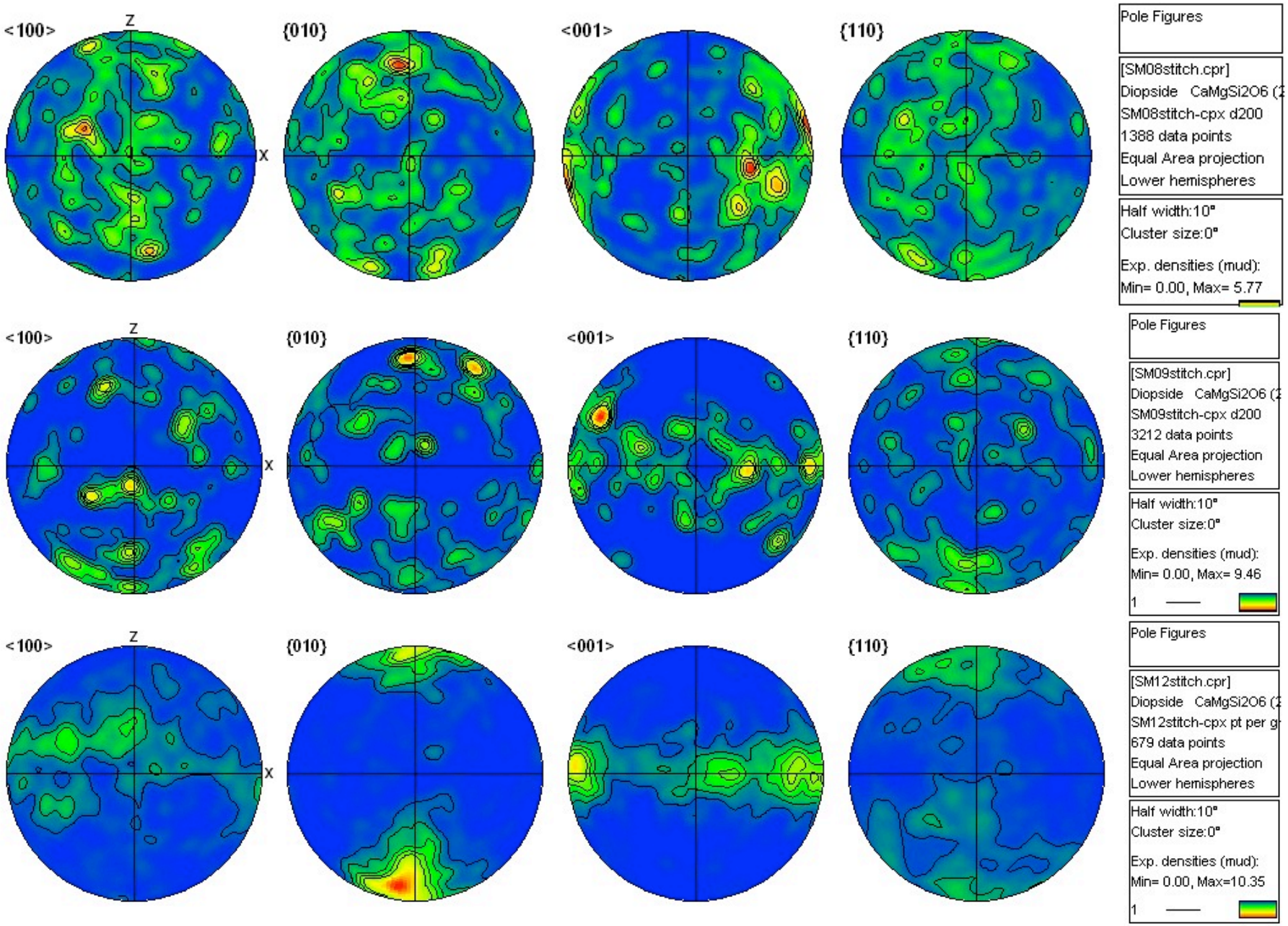
<100>
Z
X
{010}
<001>
{110}
Pole Figures
[SM08stitch.cpr]
Diopside CaMgSi2O6 (2
SM08stitch-cpx d200
1388 data points
Equal Area projection
Lower hemispheres
Half width:10°
Cluster size:0°
Exp. densities (mud):
Min= 0.00, Max= 5.77
<100>
Z
X
{010}
<001>
{110}
Pole Figures
[SM09stitch.cpr]
Diopside CaMgSi2O6 (2
SM09stitch-cpx d200
3212 data points
Equal Area projection
Lower hemispheres
Half width:10°
Cluster size:0°
Exp. densities (mud):
Min= 0.00, Max= 9.46
1
<100>
Z
X
{010}
<001>
{110}
Pole Figures
[SM12stitch.cpr]
Diopside CaMgSi2O6 (2
SM12stitch-cpx pt per g
679 data points
Equal Area projection
Lower hemispheres
Half width:10°
Cluster size:0°
Exp. densities (mud):
Min= 0.00, Max=10.35
1

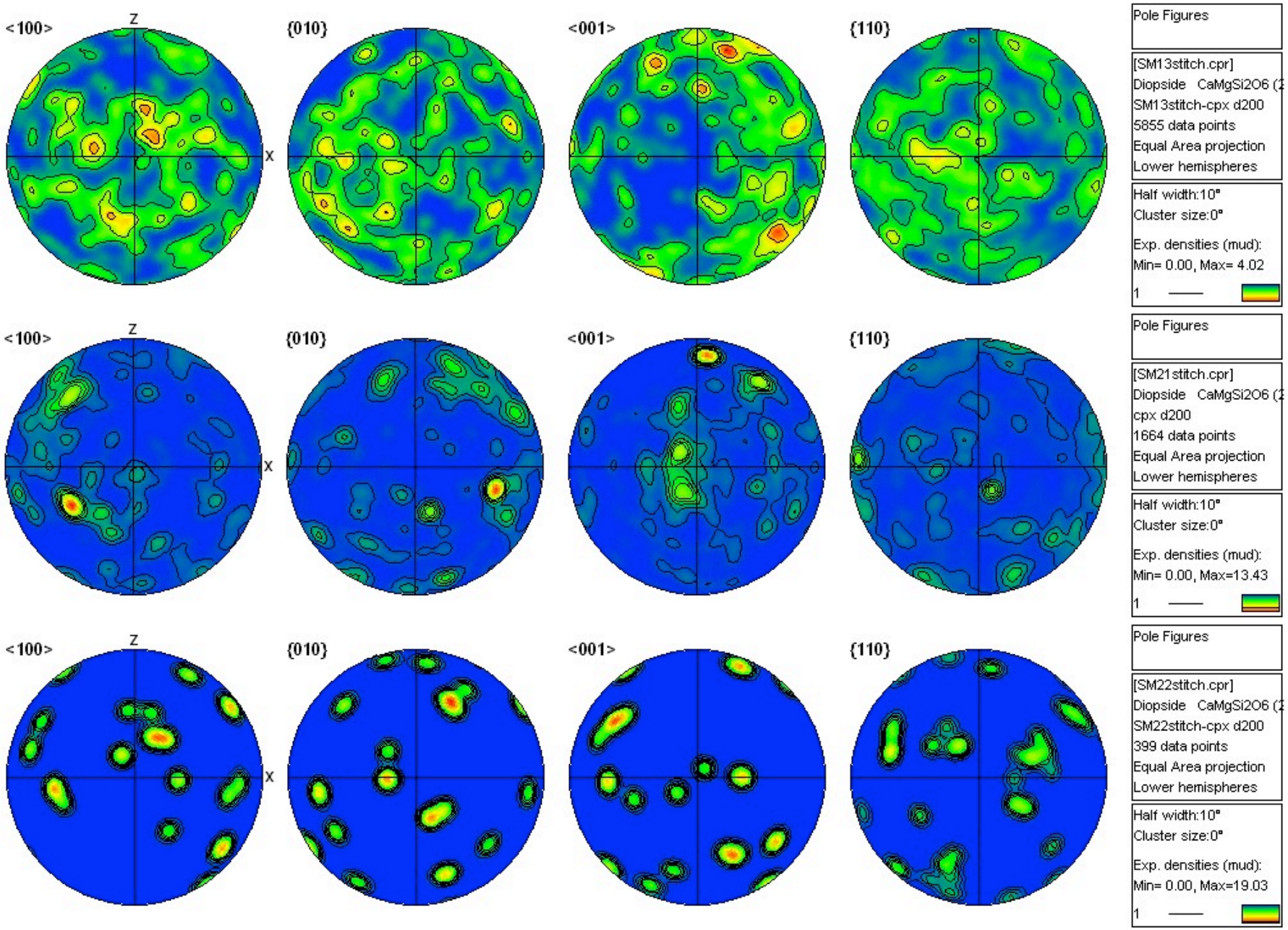
<100>
Z
X
{010}
<001>
{110}
Pole Figures
[SM13stitch.cpr]
Diopside CaMgSi2O6 (2
SM13stitch-cpx d200
5855 data points
Equal Area projection
Lower hemispheres
Half width:10°
Cluster size:0°
Exp. densities (mud):
Min= 0.00, Max= 4.02
1
<100>
Z
X
{010}
<001>
{110}
Pole Figures
[SM21stitch.cpr]
Diopside CaMgSi2O6 (2
cpx d200
1664 data points
Equal Area projection
Lower hemispheres
Half width:10°
Cluster size:0°
Exp. densities (mud):
Min= 0.00, Max=13.43
1
<100>
Z
X
{010}
<001>
{110}
Pole Figures
[SM22stitch.cpr]
Diopside CaMgSi2O6 (2
SM22stitch-cpx d200
399 data points
Equal Area projection
Lower hemispheres
Half width:10°
Cluster size:0°
Exp. densities (mud):
Min= 0.00, Max=19.03
1

Alpe Arami pole figures for diopside/omphacite